博士学位論文

Study on the hair plate proprioceptors in antennal mechanosensory system of crickets —Developmental and neuroanatomical perspectives—

（コオロギ触角機械感覚システムにおける毛板自己受容器の研究

−発生学的、神経解剖学的観点から−）

Hui Lyu

北海道大学大学院生命科学院

令和８年６月

学 位 論 文 内 容 の 要 旨

博士の専攻分野の名称： 博士(生命科学) 氏 名 呂 惠

学 位 論 文 題 名

Study on the hair plate proprioceptors in antennal mechanosensory system of crickets

—Developmental and neuroanatomical perspectives—

(コオロギ触角機械感覚システムにおける毛板自己受容器の研究 −発生学的、神経解剖学的観点から−)

コオロギやゴキブリなどの昆虫は、触角を用いて能動的に周囲の環境を走査し、障害物を知覚する。このアクティブセンシングでは、物体への接触とともに、走査している触角の位置情報が重要な手掛かりとなる。そのため、触角の基部には、毛板（hair plate）と呼ばれる機械感覚子の集合体が存在し、触角の位置や運動を脳に伝える自己受容器として機能している。これらの感覚器は、運動に伴う触角の姿勢変化を検出することで、アクティブセンシングを成立させる基盤となっている。また、これらの不完全変態昆虫では、孵化直後の幼虫もすでに触角を備え、外界を探索する行動を示す。したがって、毛板は発達初期から空間認知や運動制御に重要な役割を果たすと考えられる。しかし、毛板を構成する機械感覚子の形態や空間配置が発達に伴ってどのように変化していくのか、これまでほとんど明らかにされていなかった。

そこで本研究は、フタホシコオロギ（*Gryllus bimaculatus*）を用い、発達段階に応じた毛板の外部形態と感覚子の３次元配置、さらにそれらの求心性線維の中枢投射様式を解析し、触角機械感覚系における空間情報表現の構造的基盤を明らかにすることを目的とした。コオロギの触角は、上下の動きは頭と柄節の関節により、左右の動きは柄節と梗節

の関節で制御されており、この二つの関節がほぼ直交する単純な構造をなしている。このように、触角の動きと関節の構造の対応関係が明確であるため、ゴキブリやナナフシに比べて、触角運動と感覚入力との関係を解析しやすいという利点がある。したがって、コオロギは触角の運動制御機構や、毛板による固有受容入力の符号化を研究する上で非常に適した材料であり、アクティブセンシングの神経基盤を理解するための優れたモデル動物である。これらの特徴を踏まえ、本研究では、走査電子顕微鏡による微細構造の観察と共焦点レーザー顕微鏡を用いた三次元再構成を組み合わせ、各発達段階における毛板構造の変化を定量的に比較した。さらに、蛍光色素による神経標識法を用いて毛板感覚子の求心性線維を可視化し、中枢神経系における投射経路を明らかにした。

第一章では、成虫コオロギの触角基部に存在する毛板の形態的特徴とその三次元的配置を詳細に解析した。柄節および梗節にはそれぞれ背側・腹側・内側・外側の４箇所に毛板が存在し、個々の感覚毛の位置・長さ・本数を座標情報として定量化した。その結果、毛板の配置様式は左右対称性を保ちながら、個体間で高い再現性を示した。さらに、各毛板内部においても、感覚毛は一定の相対位置関係を保った規則的な配列を形成していた。また、各毛板の傾斜角度や配向の差から、背腹方向の毛板は触角の仰角運動、内外側の毛板は水平方向の運動に対応していることが示唆された。これらの結果は、成虫における固有受容入力の空間的基盤が、構造的に明確に分化していることを示している。

第二章では、第一章で確立した三次元解析法を用い、初齢幼虫から成虫に至るまでの発達段階における毛板構造の変化を定量的に比較した。各齢において毛板感覚子の数は段階的に増加し、脱皮による節の拡大に伴って、既存の感覚毛が保持されたまま、その間に新たな感覚子が追加されていくことが分かった。また、毛板を構成する感覚毛群の空間配置は発達段階を通してよく保存され、同一齢の個体間でも高い一致性を示した。これにより、毛板の空間的配置は遺伝的に制御されており、発達に伴うサイズ拡大の中でも感覚入力の空間分解能が維持されることが明らかとなった。さらに、感覚毛の長さ分布には発達に伴う変化が見られ、短毛と長毛が混在する構造によって、角度検出の精度が確保さ

れている可能性が示唆された。これらの結果から、毛板の発達は単なる数的増加ではなく、空間的秩序を保ちながら感覚受容特性を精緻化する過程であることが明らかになった。

第三章では、毛板感覚子の求心性線維の中枢投射を解析し、触角機械感覚運動中枢（antennal mechanosensory and motor center: AMMC）および食道下神経節（subesophageal ganglion: SOG）における神経投射様式を明らかにした。本研究では、成虫の柄節背側および梗節外側の毛板からそれぞれ異なる蛍光色素を導入して順行性二重染色を行い、脳内での軸索経路を比較した。その結果、いずれの毛板からの線維も触角葉腹側に位置するAMMCに収束し、内側に軸索側枝を分枝した後、さらに軸索は脳からSOGへ下行して終末していた。毛板の位置による投射領域の明確な差異は見られなかったが、AMMC 内の軸索側枝の形態や走行方向にはわずかな違いが認められた。これらの結果は、触角の異なる運動軸に対応する毛板入力が同一領域で統合され、運動出力に結合する仕組みを持つ可能性を示している。

以上の解析から、コオロギの毛板は発達初期から成虫まで一貫して高度に秩序化された空間配置を保持し、脱皮や成長に伴う形態変化の中でも感覚受容野を安定的に維持していることが明らかとなった。さらに、毛板感覚子の求心性線維はAMMCおよびSOGに投射し、触角運動の制御に関与する中枢神経回路の一部を構成していると考えられる。これらの結果は、昆虫の触角機械感覚系における空間情報表現の発達的および神経解剖学的基盤を明確にし、構造化された感覚入力がどのようにして文脈依存的な運動出力へと変換されるのかを理解する上で、重要な手掛かりを提供するものである。

Contents

General Introduction

Active and passive sensing

Animals employ various sensory modalities to interpret their surroundings. In general, sensory systems can be classified into these two functional modes: active sensing and passive sensing (for reviews, see Nelson and MacIver, 2006). In active tactile sensing, animals intentionally move their bodies or mechanosensory organs, while simultaneously monitoring their own movements. In other cases, animals themselves provide the energy, such as sound and electric pulses, to interact with the environment and to obtain information. In contrast, passive sensing occurs when the sensory organ remains stationary and external stimuli, such as light, sound, or chemical molecules, provide the energy that activates the receptor cells. The distinction lies in whether the animals generate the sensory energy themselves or merely receive it. When vision is unavailable, for instance, in darkness or within enclosed environments, they depend on “active sensing” as an alternative mechanism. Passive sensing, such as vision or audition, involves animals passively detecting stimuli arising from changes in the external environment. In contrast, active sensing involves animals deliberately generating sensory inputs through their own movement, action, or energy delivery. Echolocation, electrolocation, and tactile exploration are examples of active sensing to acquire spatial information (Nelson and MacIver, 2006; Engelmann et al., 2008).

My study focused on tactile sensing as a representative modality of active sensing. Nocturnal insects, such as cockroaches and crickets, move their antennae to detect the shape and location of surrounding objects and spaces (Harley et al., 2009; Ifere et al., 2022, 2025), like rodents rhythmically move their whisker to probe nearby objects and identify their position and texture (Hartmann, 2001; Prescott et al., 2011; Bush et al., 2016). These examples illustrate that active sensing is not limited to a single taxonomic group but is a widespread strategy for spatial perception across the animal kingdom.

In neuroscience, the sensory information about one's own body movements is provided by sensory feedback signals from proprioceptive organs, referred to as "reafferent," and by the efference copy of neural signals for motor control, observed as "corollary discharge" (Crapse and Sommer, 2008; Straka et al., 2018). In the whisker system, reafferent signals arise from the bending moments and high-frequency vibrations generated at the whisker base during contact with surfaces (Lottem and Azouz 2009), which are transformed into neural representations of object location and texture within the trigeminal–barrel cortex pathway (Ebert et al. 2021). Neural activity in early brainstem nuclei already exhibits a subtractive computation between reafferent and exafferent signals, indicating that sensory cancellation and predictive coding begin at the first synaptic level. At the cortical level, top-down modulation from the somatosensory cortex further gates reafferent input during active touch, allowing task-dependent control

of sensory gain (Chakrabarti and Schwarz 2018). The superior colliculus and cerebellum contribute to integrating whisker and locomotion kinematics to construct a unified estimate of self-motion and spatial position (Chinta et al. 2025; Chen et al. 2016). These findings reveal that the brain dynamically balances the suppression and enhancement of self-generated sensory inputs, ensuring perceptual stability while preserving information essential for fine spatial localization.

However, how the movements of one's own sensory organs are represented within the central nervous system and compared with external stimuli to identify precise spatial information remains poorly understood.

Kinematics of the antenna and tactile sensing in crickets

For active sensing, nocturnal insects, such as cockroaches and crickets, vigorously swing their antennae, scanning the nearby surrounding space. When the flagellum contacts an object during scanning, the contact location along the flagellum and the deflection magnitude at that contact provide information about the object distance and orientation (Okada and Toh, 2000; Ifere et al., 2022, 2025). In addition, tactile interactions between the flagellum and object surfaces convey information about surface properties, such as texture and stiffness (Comer et al., 2003; Loudon et al., 2014). Continuous changes in this information during antenna scanning also allow for the detection of the

contour or spatial arrangement of objects. Since the flagellum has no intrinsic musculature (Honegger et al., 1990; Allgäuer and Honegger, 1993), the active antennal scanning is generated by movements of the basal joints to sample their surroundings. These active tactile sensing guides localization, navigation, and collision avoidance, particularly under conditions where visual input is limited (Okada and Toh, 2000; Ritzmann et al., 2012; Ifere et al., 2022, 2025).

Crickets are useful models for studying insects' active mechanosensory systems because the kinematics of their antennae are structurally simple and experimentally tractable (Staudacher et al., 2005). Each antenna consists of three parts: a scape, a pedicel, and a flagellum, which are connected by two joints positioned at nearly right angles to one another. The pedicel–scape joint generates mediolateral movements in the horizontal direction, and the head–scape joint controls dorsoventral elevation in the vertical direction. These two rotational axes form a geometric system that can be described within a three-dimensional coordinate frame (Baba and Comer, 2008). This articulation provides the mechanical basis for tactile exploration. Because the simple mechanical architecture of the cricket antenna is straightforward and the associated behaviors are stereotyped, this system would be useful for exploring how tactile information is acquired at the periphery and supports spatial perception and motor control.

In antennal mechanosensing as allocative sensing, the cricket must continuously monitor the position of its antennae at every moment during scanning to accurately determine the position of contacted objects. However, how proprioceptive information about antennal position is provided to the nervous system, and which peripheral receptors contribute to this process remain unclear.

Goal of this thesis

The central goal of this thesis is to clarify how the antennal hair plates located at the scape and pedicel joints function as proprioceptive mechanosensors and to identify target areas to which they provide sensory feedback about antennal position and movement. Because crickets rely on antennal active sensing from early post-embryonic stages, effective proprioceptive feedback must be maintained despite substantial growth and repeated molting. Therefore, understanding how the spatial organization of hair plates is established and preserved during development is essential for explaining the functional stability of antennal proprioception. To achieve these objectives, I have integrated morphological, developmental, and neuroanatomical analyses of them.

Chapter 1 describes the basic structure of hair plates at the antennal base. I have built a clear three-dimensional framework of the hair plates. This framework showed the actual positions and patterns of the hair plates on the joint surface. In this chapter, using

scanning electron microscopy (SEM), I first examined the external morphology of the antennal base. The high-resolution SEM images were used to identify the position, size, and shape of each hair plate group. Each mechanosensory sensilla, joint membranes, and surrounding bristles were distinguished. Next, I used confocal laser scanning microscopy to make a 3D reconstruction of the antennal base. After removing internal tissues and keeping only the cuticle, I obtained continuous optical slices of the cuticular autofluorescence. Based on these confocal optical slices, I reconstructed the 3D outline of the antennal base, revealing structural features of the four hair plate groups and their relationships to joint axes. These observations allow us to create a 3D map of the hair plates. This map was used as a spatial reference for the developmental analysis in Chapter 2 and helped explain how hair plates encode joint angle.

Chapter 2 focused on the developmental changes of the hair plates. The main question of this chapter was whether the spatial arrangements of antennal hair plates identified in adult crickets were maintained during nymphal stages. To answer this question, I performed the same analysis used in Chapter 1 on the crickets from the first instar through adulthood. I counted the sensilla, examined their arrangements, and measured the nearest-neighbor distances for each hair plate. I also measured sensillum length and tested relationships between the sensillum length and its location. I found that new sensilla emerged at a specific position, suggesting the presence of developmental

rules. Through these analyses, possible developmental mechanisms that support the stability in the distribution of sensilla were proposed.

In Chapter 3, I analyzed the central projections of sensory afferents from antennal hair plates to clarify how proprioceptive information is conveyed to the central nervous system. Anterograde labeling of sensory afferents of different hair plates revealed the projection pathways of them in the brain and subesophageal ganglion. Afferents from all hair plates converged in the antennal mechanosensory and motor center (AMMC) and extended further to the subesophageal ganglion, although no clear segregation of projection areas was observed among hair plates at different positions. However, subtle differences were found in the branching patterns and trajectories of axonal collaterals within the AMMC. These anatomical results suggest that proprioceptive inputs from hair plates associated with different axes of antennal movement are integrated within a common central region and are likely coupled to motor output during active tactile sensing.

Chapter 1: Morphology and three-dimensional reconstruction of the antennal base

1.1 Introduction

When visual perception is limited, such as in dark or enclosed spaces, many animals rely on active sensing to navigate their surroundings and detect obstacles. For insects, active tactile exploration using the antennae plays a crucial role in spatial perception independent of the visual system. Antennal mechano-sensing mediates object detection and route guidance during obstacle negotiation behaviors in cockroaches (Harley et al., 2009) and stick insects (Krause and Dürr, 2012). In crickets, antennal mechanosensory inputs modulate cercal-mediated escape behavior depending on the shape and position of obstacles, indicating that antennal inputs provide spatial cues that can be used for behaviors elicited by other sensory systems, although they do not necessarily trigger those behaviors directly (Ifere et al., 2022, 2025).

In the insect antennal system, the basal segments are actively moved by muscles at the scape-pedicel (SP) and head-scape (HS) joints, whereas the flagellum lacks intrinsic musculature (Honegger et al. 1990). Mechanosensory receptors located on the scape and pedicel predominantly function as proprioceptors, which provide sensory feedback about antennal position and movements (Toh, 1981). Tactile stimulation of the antennal

flagellum elicits the escape response in cockroaches, which is also triggered even if the flagellum is replaced with an artificial object. (Comer et al., 2003). This means that the basal segments of the antenna provide not only self-generated feedback signals but also sensory inputs generated by external stimuli. Thus, the function and organization of mechanoreceptors at the antennal base need to be investigated for understanding the neural substrate of antennal active sensing.

Abundant exteroceptive bristles are distributed at the base of the antenna, as well as proprioceptors, such as the internal Johnston's organ (JO), external campaniform sensilla (CS), and hair plates (also referred to as Böhm's bristles) (Staudacher et al., 2005). JO is located beneath the cuticle at the flagellum–pedicel junction and responds to vibratory stimuli, triggering escape responses (Comer and Baba, 2011). CS, arranged in a circular pattern on the distal pedicel, detect cuticular strain and deformation generated at the flexible connection between the pedicel and flagellum (Pringle, 1938; Toh, 1981). Hair plates are distributed on the surfaces of both the scape and pedicel and are thought to be principal proprioceptive sensors precisely detecting antennal position (Okada and Toh, 2000, 2001). However, the three-dimensional positions of individual mechanoreceptive hairs relative to the joint geometry, as well as the presence of any spatially ordered relationship between sensillar length and location within each hair plate,

have remained unknown. The findings on these issues will provide crucial insights into how the hair plate detects and encodes antenna orientation.

To address these issues, I used the field cricket *Gryllus bimaculatus* as a model animal. In this species, dorsoventral movement of the antennae is achieved through the horizontal axis of the HS joint, whereas mediolateral movement is controlled by the vertical axis of the SP joint. These two axes form an orthogonal articulation that allows basic but effective control of the antennal direction (Staudacher et al., 2005). This organization means that crickets‘antennal kinematics are simpler than those in cockroaches and stick insects (Okada and Toh, 2004; Kraus and Dürr, 2004).

To understand how hair plates detect joint movements, it is necessary to know their three-dimensional (3D) locations around the antenna base. Most previous studies have described them in two dimensions, so a systematic spatial reconstruction remains lacking. In this chapter, I used scanning electron microscopy and confocal microscopy to make a 3D image of the antennal base and identify the dorsal, ventral, medial, and lateral hair plates. I also measured the external structure of individual sensilla and analyzed the relationship between their arrangement and length.

These structural data provide the morphological basis for the developmental analysis in Chapter 2 and the central projection study in Chapter 3. They also help explain how crickets sense the angles of antennal joints during active tactile exploration.

1.2 Materials and Methods

Animals

A wild-type strain of the field cricket *Gryllus bimaculatus* DeGeer (Hokudai WT strain; Watanabe et al., 2018) was used in all experiments. The animals were reared in laboratory on an artificial mouse diet (Oriental Yeast Co., Tokyo, Japan) with water provided ad libitum, under a 12:12 h light/dark cycle at a constant temperature of 27 ˚C. Adult male crickets less than seven days post-imaginal molt were used for all analyses. Only individuals with intact and undamaged antennae were selected for further analysis to ensure accurate morphological measurements. According to the guidelines of the Institutional Animal Care and Use Committee of the National University Corporation, Hokkaido University, Japan, no requirements were applicable for insect treatment in these experiments.

Scanning electron microscopy

Crickets were anesthetized by cooling on crushed ice and then decapitated. The removed heads were soaked in 50% acetone and cleaned using an ultrasonicator (Iuchi US-1; SND, Japan) for 15 minutes. Subsequently, the specimens were dehydrated in an ascending series of acetone solutions (50%, 70%, 90%, and 100%; 5 min each), air-dried, and coated with gold using an ion sputterer (E-1045; Hitachi, Japan). The pretreated

specimens were imaged using a field-emission scanning electron microscope (S-3000N; Hitachi, Tokyo, Japan) at an accelerating voltage of 5–10 kV.

Three-dimensional reconstruction of the antennal basal segment

To remove all tissues except the cuticle, the basal segment of the antenna was isolated and immersed in 1 N NaOH at 60 ℃ for 24 h. After treatment, the specimens were dehydrated through a graded ethanol series (50%, 70%, 90%, and 100%) and then cleared in methyl salicylate. The transparent samples were mounted in a drop of Bioleit reagent (Okenshoji, Tokyo, Japan) on a concave glass slide to preserve their three-dimensional structure. The cuticles of the basal segment exhibited strong autofluorescence in the green-to-yellow color range when illuminated with a 488 nm laser line. Optical section images were acquired at 1 μm Z-steps using a confocal laser scanning microscope (LSM980, Zeiss) equipped with a 10× dry objective (Plan-Apochromat 10×/0.45 M27, Zeiss). Each optical slice was captured at a resolution of 1024 × 1024 pixels (pixel size 0.83 μm × 0.83 μm). Multiple images of a single specimen were seamlessly stitched in *ImageJ* (version 1.54; Schneider et al., 2012) to reconstruct a complete three-dimensional model of the antennal base. Morphometric parameters were measured from the reconstructed confocal images (n = 3 individuals) in *ImageJ* (version 1.54).

Data analysis

All statistical analyses and data visualizations were performed in *R* (version 4.5.0; R Core Team, 2025). For each sensillum, the measured length value ($L_{\text{sensillum}}$) was normalized by the length of the corresponding basal segment to obtain a dimensionless normalized value, as defined below:

$$L_{\text{norm}} = \begin{cases} \frac{L_{\text{sensillum}}}{L_{\text{scape}}}, for\ dorsal\ and\ ventral\ regions \\ \frac{L_{\text{sensillum}}}{L_{\text{pedicel}}}, for\ medial\ and\ lateral\ regions \end{cases}$$

To classify individual sensilla based on their normalized length, a K-means clustering algorithm was used. The number of clusters was determined using the silhouette method. For each hair plate, clustering solutions with different k value were evaluated, and the k value that maximized the mean silhouette width was selected as the optimal number of clusters.

Based on this criterion, two clusters (k = 2) were consistently supported across all hair plate regions. Two classified clusters were automatically ordered by their mean center values and designated as “short” and “long”.

1.3 Results

Morphological features of the hair plates at the antenna base

Scanning electron microscopy (SEM) revealed the fine structural organization of the antennal base in *Gryllus bimaculatus*. The basal segments comprise the scape and pedicel, which serve as the foundation for antennal movements (Fig. 1-1A). High-magnification SEM images showed clusters of hair plate sensilla on the posterior surface of the scape (Fig. 1-1B), while similar groups of sensilla were also observed on the corresponding articular surface of the pedicel (Fig. 1-1C).

Detailed observation of a single sensillum on the scape revealed that each hair plate sensillum was embedded within a flexible socket structure located directly on the joint surface (Fig. 1-2A; Toh, 1981). The sensilla were located in direct contact with the articular membrane at the basal joints (Fig. 1-2B), indicating that they could be deflected by adjacent membranes when the antennal segments moved relative to each other. This anatomical arrangement suggests that the hair plates are structurally adapted to detect small relative movements between the scape and pedicel, thereby providing precise mechanosensory feedback on antennal orientation.

Three-dimensional reconstruction of hair plate distribution

To further investigate the spatial organization of hair plates, I created three-dimensional reconstructions of the antennal base, based on confocal microscopic images (Fig. 1-3). Four groups of hair plates were consistently observed across individuals: the dorsal, ventral, medial, and lateral groups. The dorsal and ventral hair plates were located on the proximal surface of the scape, which were thought to detect dorsoventral movements of the antenna. The medial and lateral hair plates were located on the proximal surface of the pedicel and are associated with detecting mediolateral swing of the antenna.

Classification of sensilla length and spatial distribution

To characterize variation in sensillar morphology, the normalized lengths of sensilla from all four hair plates were analyzed using a K-means clustering algorithm with $k = 2$. The sensilla were classified into two statistically distinct length groups: short and long (Fig. 1-4A). These two length groups were not randomly distributed within a hair plate. Short sensilla were basically located near the proximal or medial margins, where they lie closer to the pivot of the joint. Long sensilla were usually positioned distally or along the lateral edges of the plate, farther from the axis of rotation (Fig. 1-3).

SEM observations showed clear intermingling of sensilla with different lengths on both the scape (Fig. 1-4B) and the pedicel (Fig. 1-4C), supporting the results of 3D reconstruction. Although this spatial pattern suggests that sensilla of different lengths may have different angular response ranges, the evidence in this chapter is not sufficient to support this functional interpretation. To verify this hypothesis, it is necessary to analyze the relationship between sensillum length and its distance from the joint center. These quantitative data are presented in the adult datasets in Chapter 2 (Fig. 2-3, 2-4, 2-5, 2-6).

Kinematics of the antenna

Movements at the head–scape (HS) and scape–pedicel (SP) joints generated two primary and orthogonal axes of rotation of the antenna. The HS joint mediated dorsoventral movements of the antenna, while the SP joint controlled mediolateral movements (Fig. 1-5A–D). These two rotational degrees of freedom together appeared to form the fundamental mechanical basis of antennal movements, as shown in schematic diagrams of joint geometry (Fig. 1-5E, F). During dorsoventral rotation at the HS joint, the antenna flagellum moved together with the scape and pedicel. Likewise, mediolateral rotation at the SP joint produced lateral movements of the pedicel and distal flagellum, but the scape was immobile relative to the head capsule. The four hair plates positioned

along these joint surfaces probably detect small displacements of the cuticular membrane during rotation by contacting and deflecting the sensilla.

1.4 Discussion

Three-dimensional spatial organization of antennal hair plates

In this chapter, I examined the detailed spatial arrangements of antennal hair plates based on 3D reconstruction of the antennal base of *Gryllus bimaculatus*. The head–scape (HS) and scape–pedicel (SP) joints operate along two orthogonal axes that separately control vertical and horizontal antennal movements, respectively (Staudacher et al., 2005). The four hair plates (dorsal, ventral, medial, and lateral) were consistently positioned along these joint surfaces in a geometry that directly corresponds to the two movement axes. The dorsal and ventral hair plates were located along the proximal surface of the scape, aligned with the axis of dorsoventral movement, whereas the medial and lateral hair plates were positioned on the pedicel surface associated with mediolateral movement. This tight geometric coupling suggests that these hair plates are optimized to detect rotation around a specific axis.

Anatomical features revealed by the 3D reconstruction indicate that the mechanoreceptors were mechanically well-positioned to detect angular changes during antennal movements. The simple, orthogonal joint structure and suitable alignment between joint kinematics and sensilla placement likely provide a direct physical foundation for hair plate afferents to monitor antennal orientation with high fidelity and

to provide precise proprioceptive information about antennal movements during active sensing.

Functional implementation in sensillar distribution

In this chapter, I observed that sensilla with different hair lengths tended to occupy characteristic positions within each hair plate. The length of each sensillum is thought to determine its sensitivity to the joint angle. Although mechanical sensitivity is also influenced by material properties such as stiffness, sensillum length represents the most directly observable morphological factor in the present analysis. Short sensilla, located closer to the joint pivot or inner margin of the plate, are likely to be deflected by smaller angular displacements. Longer sensilla, positioned farther from the pivot or near the outer boundary of the hair plate, would require larger movements for activation. This arrangement probably allows the hair plate system to provide proprioceptive signals about the joint angle by gently graded recruitment of sensilla as the joint rotates. This estimation aligns with previous physiological studies showing that hair plate receptors exhibit phasic–tonic responses to antennal deflection (Okada & Toh, 2001) and with computational work indicating that sequential recruitment of individual sensilla can encode joint angle (Ache & Dürr, 2015). Thus, the spatial arrangement of hair plate

sensilla based on sensillar length likely supports proprioceptive monitoring of antennal orientation, enabling crickets to identify contacting objects through active sensing.

Antennal movement encoding predicted by sensillar arrangements and antennal kinematics

Antennal movements can be predicted based on sensory information about the HS and SP joint rotations during dorsoventral and mediolateral deflections of the antenna flagellum. Since hair plates were positioned along the corresponding joint surface, antenna rotation would bring the adjacent cuticular membrane into contact with the hair plate at specific orientations. By combining the sensory inputs about the rotational axis and each joint angle, the central nervous system should calculate the precise orientation of the antenna during active antennal scanning. If so, the next biological question is how the postsynaptic circuits in the central nervous system decode the information about the antennal joint angle and rotational axis. Spatial information of mechanosensory inputs is often represented by topographic organization (Jacobs and Theunissen, 2000; Ogawa et al., 2008). To address this question, I examined central projections of sensory afferents from hair plate sensilla in Chapter 3.

1.5 Figures

(Figure 1-1)

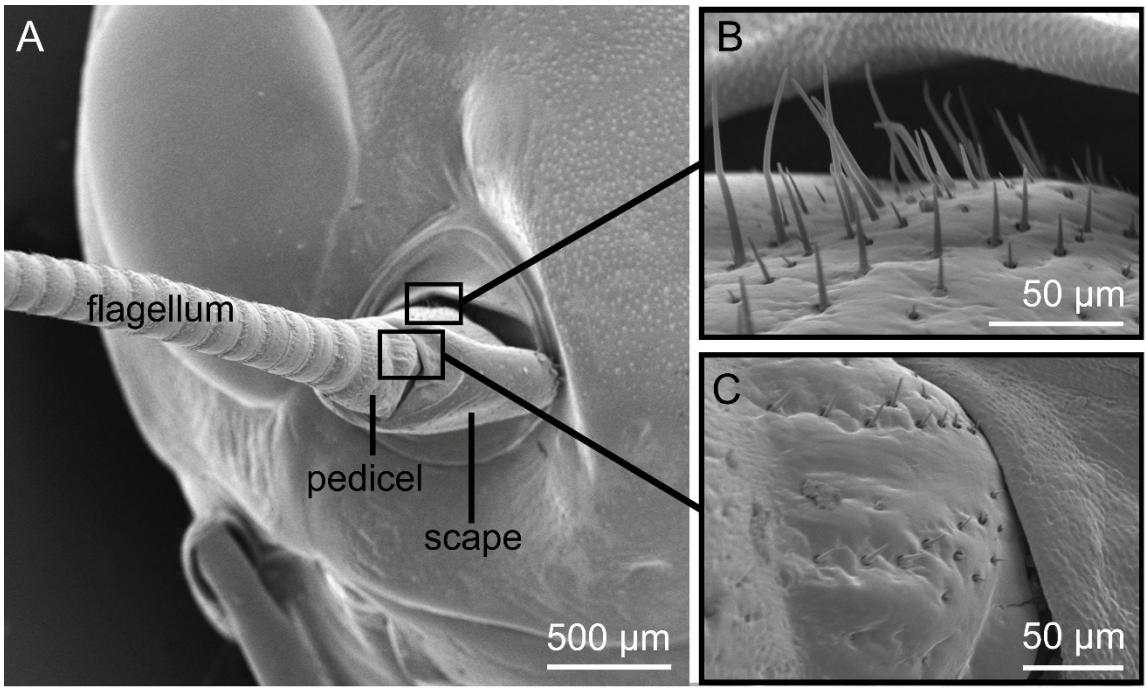

Figure 1-1. Scanning electron micrographs of the antennal base segments of *Gryllus bimaculatus*.

(A) Frontal view of the cricket head showing the scape, pedicel, and filamentous flagellum. **(B, C)** Higher-magnification views of the scape (B) and pedicel (C).

(Figure 1-2)

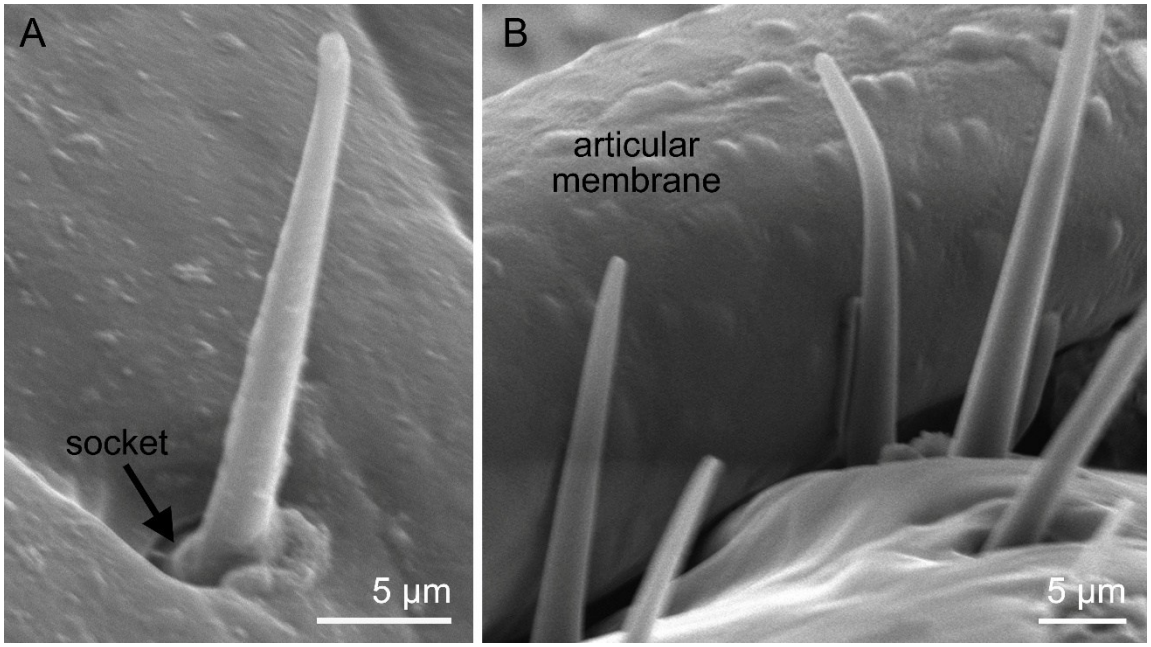

Figure 1-2. Scanning electron micrographs of the hair plate sensilla.

(A) A single hair plate sensillum on the scape, embedded in a flexible socket at the joint surface. **(B)** Hair plate sensilla deflected by the adjacent articular membrane.

(Figure 1-3)

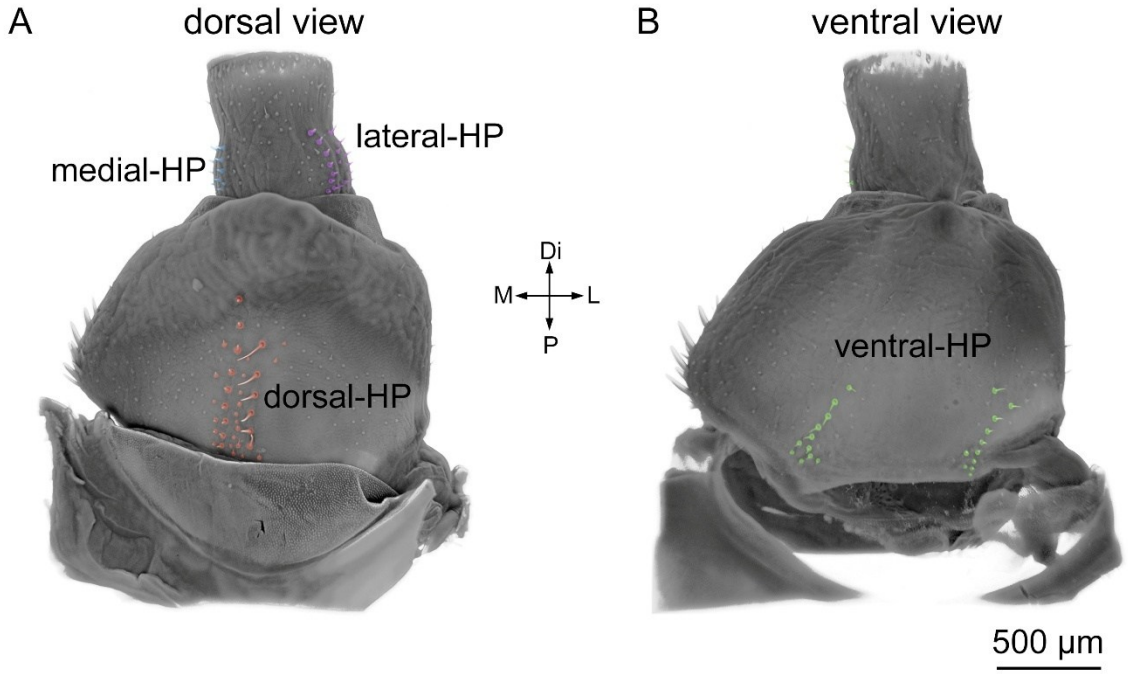

Figure 1-3. Three-dimensional reconstructed the antennal base and spatial distribution of hair plates.

(A, **B)** Dorsal (A) and ventral (B) views of antennal base in adult crickets. Sensilla of the medial, lateral, dorsal, and ventral hair plates (HP) hair plates were colored in cyan, purple, orange, and green, respectively. Di, distal; P, proximal; M, medial; L, lateral.

(Figure 1-4)

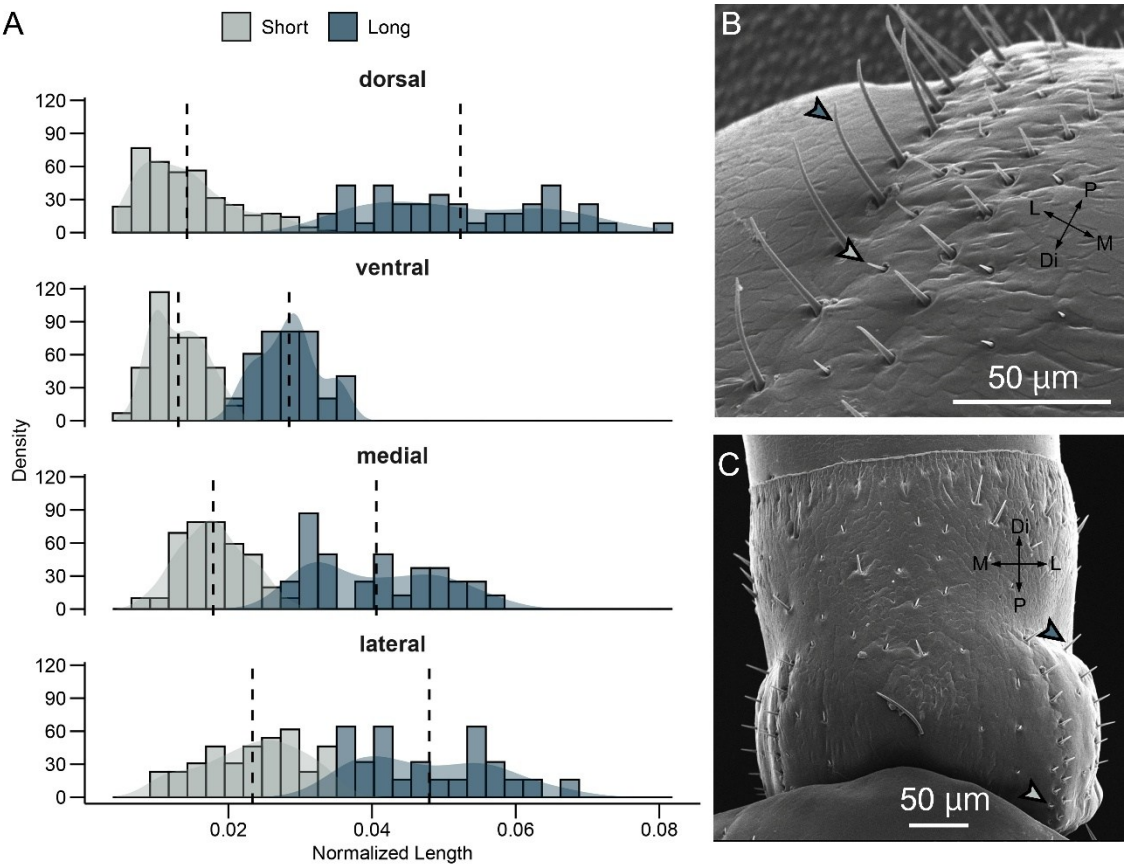

Figure 1-4. Distributions of hair plate sensilla with varying hair length.

(A) Normalized hair lengths of each mechano-sensillum in four (dorsal, ventral, medial, and lateral) hair plates. The sensilla were classified into 2 groups (short and long) using a K-means clustering algorithm. The shades indicate kernel density curves for the distribution of normalized lengths for each hair plate. Dashed lines indicate the cluster centers. **(B, C)** Scanning electron micrographs of the dorsal hair plate on the scape (B) and the dorsal surface of the pedicel (C), including the medial and lateral hair plates shown by arrowheads. The colors of arrowheads correspond to the hair length groups.

(Figure 1-5)

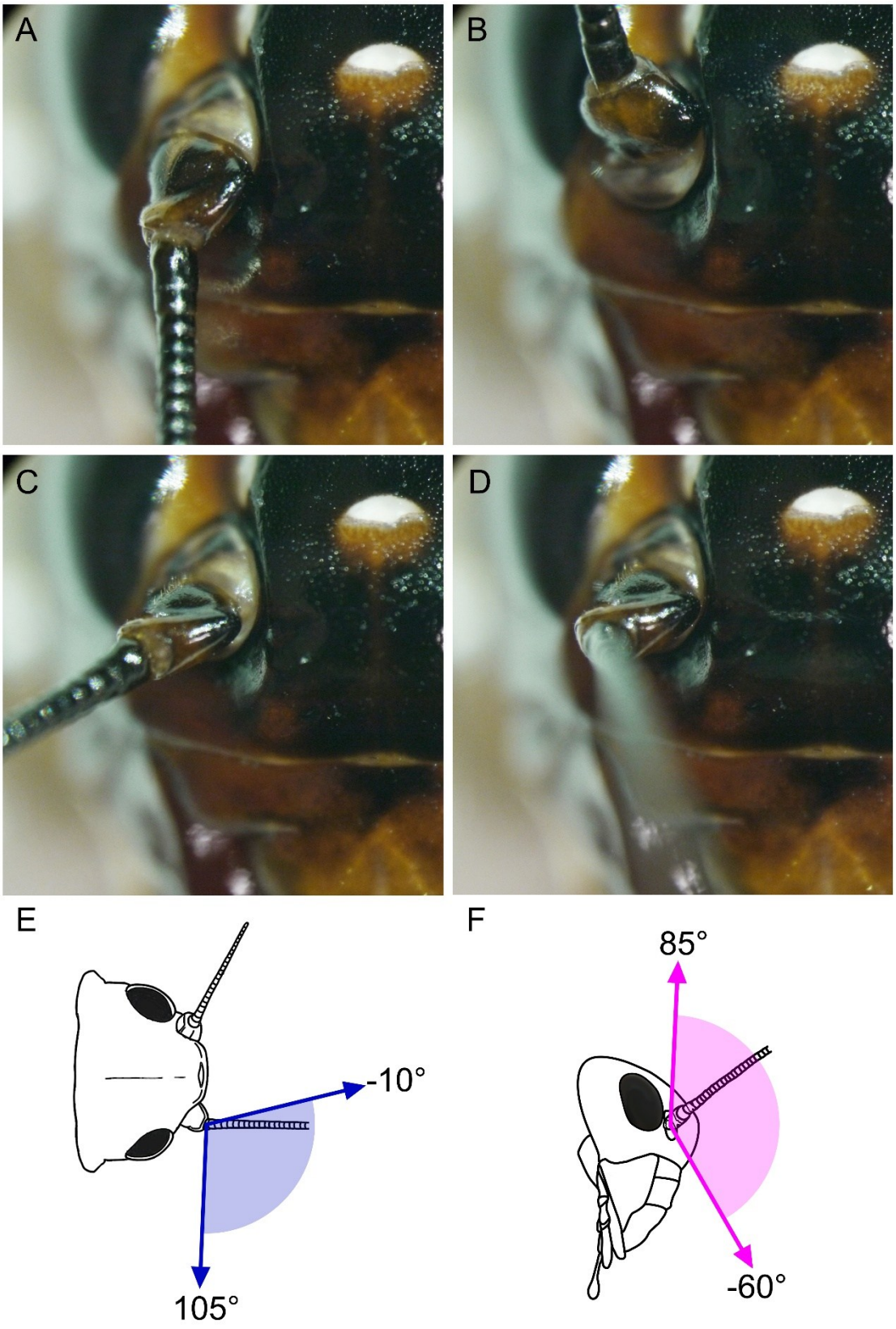

Figure 1-5. Horizontal and vertical movements of antenna.

(A–D) Sequential images of the right antennal base during ventral (A), dorsal (B), lateral (C), and medial (D) deflections of the antenna. **(E, F)** Schematic diagrams illustrating the horizontal (mediolateral) movements around the vertical axis of the SP joint (E) and vertical (dorsoventral) movements around the horizontal axis of the HS joint (F). Color shades indicate the angular range of antennal movements. The anterior direction, parallel to the body axis, was defined as 0º in the horizontal plane, with the lateral rotational direction being positive. The horizontal direction of the body axis was defined with 0º in the vertical plane, with upward elevation being positive.

Chapter 2: Developmental pattern formation and spatial organization of antennal hair plates

2.1 Introduction

The spatial organization of antennal hair plates is essential for detecting basal joint angles that determine the orientation of the antenna flagellum during active tactile sensing. Crickets, which are hemimetamorphic insects, possess antennae even in their newly hatched nymphal stage and perform active sensing via these antennae throughout their developmental period. Effective proprioceptive inputs require the orderly arrangement of mechano-sensilla on the scape and pedicel observed in adult crickets in Chapter 1, which must be maintained throughout the post-embryonic growth process. However, it remains unclear whether this spatial pattern is developmentally conserved during substantial morphological changes across nymphal stages.

The development and molting-associated renewal of mechanoreceptors have been documented in various hemimetabolous insects. In cockroaches, ultrastructural investigations revealed that campaniform sensilla undergo a cyclic loss and reconstruction of their sensory processes at each ecdysis, demonstrating that the mechanotransduction apparatus is periodically rebuilt rather than continuously maintained (Moran, 1971; Moran et al., 1976). Complementary morphological studies

further showed that antennal postembryonic development proceeds through the sequential addition of new sensilla while maintaining the species-specific adult pattern of sensory organ distribution (Schafer and Sanchez, 1973; Schafer, 1997). In stink bugs, quantitative analyses of antennal sensilla showed a progressive increase in sensillum number across nymphal stages, while sensillum types remained consistent during development (Brézot et al., 1996). Similar molting-associated renewal of mechanoreceptive hair sensilla has been described in silverfish and bristletails, where mechanosensory hairs are replaced at each molt without disrupting the overall organization of the sensory array (Thomann et al., 1997). In mantids, flagellomere development exemplifies the complexity of antennal growth in hemimetabolous insects, with multiple processes jointly expanding segment number and sensory capacity (Carle et al., 2014). In stick insects, the subgenual organ complex is already differentiated and functional at hatching, with later development limited to adjustments in sensillar orientation that refine vibration sensitivity (Strauß, 2024).

In crickets, the developmental processes of mechanoreceptors have been well studied in the cercal organ, where various types of mechanoreceptors are distributed (Gnatzy and Schmidt, 1971; Gnatzy, 1978). During each molting, the old cuticle detaches from the epidermis, and a new cuticle, including sensory structures, forms beneath it (Gnatzy and Römer, 1980). The ventromedial array of cercal clavate hairs, which detects

gravity acceleration, shows a consistent spatial position of each sensillum. The sequential addition of sensilla across instars yields a highly stereotyped pattern, enabling each receptor to be individually identified based on its position (Murphey et al., 1980). In contrast to the cercal sensilla, the developmental trajectory of the spatial organization of antennal hair plates remains unknown. Could the precise arrangement of hair plate sensilla required for effective tactile sensing be established during development?

Considering the function of antennal hair plates as proprioceptors, morphological features, including their spatial arrangements and sensillar distribution correlated with each hair length, are estimated to be consistent across individuals throughout the developmental stage, suggesting genetic regulation of them. If the basic spatial layouts are maintained throughout development, what lengths of new sensilla are added, and where, as the hair plate expands during the cricket's growth? Furthermore, it would also suggest that the essential parts of the central sensory circuit processing these proprioceptive inputs are already formed during the nymphal stage.

In this chapter, I investigated the developmental changes in the spatial organization of antennal hair plates from the first instar to adulthood. The specific questions in this chapter are as follows: 1) What lengths of new sensilla are added where? 2) Are the spatial features of hair plate arrangements preserved throughout development? 3) Does the position of the hair plates shift relative to the expanding antennal base? The

answers to these questions will provide valuable cues for understanding how antennal proprioception maintains functional stability throughout development.

2.2 Materials and Methods

The Methods for *Scanning electron microscopy* and for *Three-dimensional reconstruction of antenna basal segment* were identical to those in Chapter 1.

Animals

A wild-type strain of crickets (*Gryllus bimaculatus* DeGeer, Hokudai WT strain) reared in laboratory was used in all experiments. All animals were reared in a 12:12 h light/dark cycle at a constant temperature of 27 ℃ throughout development. Crickets at various stages, which were nymphal instars N1–N8 and adults < 1-week post-imaginal molting, were used to investigate developmental changes in mechanosensory hair plates. The developmental stage of nymphs was determined based on external morphological features, such as body size and wing pad development, as described in a previous study (Suzuki and Nishimura, 1997). Only individuals with intact and undamaged antennae were chosen for analysis to ensure morphological measurements of antennal hair plates. From the sixth instar onward, when sex could be reliably identified by the presence of female ovipositors, only male crickets were used for all experiments. The guidelines of the Institutional Animal Care and Use Committee of the National University Corporation, Hokkaido University, Japan, do not specify any specific treatment requirements for insects in experiments.

Morphological measurements of the antennal basal segment

The number and length of mechanosensilla on the hair plate were measured in 3D-reconstructed images by using a confocal microscope (LSM980, Zeiss, Oberkochen, Germany). The 3D images were obtained through the same procedure described in Chapter 1 for each developmental stage. Morphometric parameters, including the length and number of sensilla, were measured from reconstructed images. For all developmental stages (N1–N8 and adults), these morphometric parameters and the spatial distribution of the sensilla were determined for four different positions of hair plates (dorsal, ventral, medial, and lateral) (n = 5 individuals for each stage).

Data processing

Three-dimensional locations of individual hair plate sensilla were determined based on the confocal images and organized for each specimen. Thus, the original morphological parameters consisted of the three-dimensional coordinates (X, Y, Z) describing the spatial position of each sensillum. For spatial alignment and dimensionality reduction of the morphological parameters, principal component analysis (PCA) was used in R (version 4.5.0; R Core Team, 2025). PCA was applied primarily to align the coordinate systems across samples by identifying the major axes of spatial

variation, rather than to reduce the number of measured spatial dimensions. Three-dimensional coordinates for each sensillum were centered by subtracting the mean position of all sensilla in each hair plate, and then PCA was performed using the built-in prcomp function to derive the major axes of spatial variation. The coordinate data of the sensilla were projected onto these principal axes, which were X_pca and Y_pca, enabling comparison of the sensilla distribution pattern across different samples and stages. Spatial similarity in the distribution of sensilla between samples was quantified using pairwise Hausdorff distances (Alt et al., 2003) computed with the NumPy (Harris et al., 2020) and SciPy (Virtanen et al., 2020) libraries in Python (version 3.13).

2.3 Results

Morphological features of the antennal base segments in nymph

Using a scanning electron microscopy (SEM), I observed the ventral side of the scape in the second and fourth instars, comparing to the adults. The hair plate sensilla in the nymph were also arranged in two rows at the base of the HS joint, just like those in adults, revealing that the stereotyped and orderly spatial arrangement of sensilla is maintained throughout development (Fig. 2-1A–C). However, the position of the hair plates appeared to shift toward the proximal end of the scape as development progressed. The position of the hair plates gradually shifted toward the proximal end of the scape as the developmental stage progressed. This positional shift might indicate a developmental adaptation that helps these hair plates precisely detect the movements of antennal segments, even as body size increases. Confocal image of the antennal base during the final molt showed that the hair plate sensilla for the adult were prepared at the same position as the final nymphal stage (Fig. 2-1D). In addition to them, additional new sensilla seemed to be produced at a more distal region from the joint base. These results indicated that the relative positions and orientations of sensilla were preserved, suggesting that the spatial layout of the hair plate is maintained throughout development.

Three-dimensional distribution of the hair plate

To further investigate the detailed spatial organization of hair plates, I created three-dimensional reconstructions of the antennal base across various developmental stages, based on confocal microscopic images (Fig. 2-2). Four distinct groups of hair plates were consistently observed across individuals and developmental stages: the dorsal, ventral, medial, and lateral groups. The dorsal and ventral hair plates are located on the posterior surface of the scape, which were thought to detect dorsoventral movements of the antenna. The sensilla of the dorsal hair plate were arranged linearly in two to several rows adjacent to each other in the proximal-distal direction, while the sensilla of the ventral hair plate were arranged in two rows separated from each other (Figs. 2-3, 2-4). Meanwhile, the medial and lateral hair plates are located on the posterior surface of the pedicel, which likely detect mediolateral movements of the antenna. These hair sensilla were also arranged in a few rows, from proximal to distal (Figs. 2-5, 2-6). These stereotyped and region-specific arrangements of the hair plate sensilla on the scape and pedicel were already observed at the first instar, suggesting that this spatial distribution was conserved throughout development.

Moreover, to quantify developmental changes in the arrangement of sensilla as the antennal base segments grew, I compared the spatial patterns of their locations by normalizing the hair plate size (Figs. 2-3, 2-4, 2-5, 2-6). As the developmental stage

progressed, the number of sensilla for each hair plate increased. By adding new sensilla at specific locations, the sensilla cluster of each hair plate expanded without altering the overall spatial pattern. The sensilla within each hair plate were distributed in a compact, constrained area, and their relative positions appeared to stay consistent across developmental stages. Even as the number of sensilla increased, their arrangement maintained the original shape and direction for each plate. In the dorsal hair plate, two distinct rows of sensilla were observed from the N1 to N3 instars. In the N4 instar, the third row of sensilla began to appear between the previous two rows, and in the N5 instar, this row became more prominent. In the N6 instar, a fourth row of sensilla appeared along the medial edge of the dorsal hair plate, toward the midline of the antenna. In contrast, the ventral hair plate maintained a two-row layout throughout development, although in the instars older than the N6 stage, additional short sensilla appeared close to the proximal region. The medial and lateral hair plates exhibited almost symmetrical and similar arrangements of sensilla. In instars older than the N6 stage, a third row of shorter sensilla developed between the previous two rows on these hair plates. This three-dimensional organization conserved across development suggests that hair plate placements are genetically regulated and that the mechanosensory system maintains its functional topology despite substantial size increases during maturation. The alignment of hair plate positions with the major axes of antennal movements is effective for detecting specific

directional displacements, suggesting their roles in proprioceptive feedback in cricket antennae.

Developmental dynamics and morphometrics of antennal basal segments

To elucidate developmental changes in antennal hair plates, I examined their morphometric parameters, such as the size and number of sensilla in four regions of the basal segments, across different developmental stages. For quantitative analysis of the development in basal segment size, I measured the straight-line distance between the proximal and distal ends of each segment, based on 3D confocal image data. Both the scape and pedicel rapidly increased in the proximal-distal length throughout development, from the first instar (N1) to the adult stage (Fig. 2-7A, Table 2-1). Notably, the segment length showed a significant increase from the fifth to seventh instars (N5–N7). On the other hand, the nearest-neighbor distances between sensilla increased almost linearly in all four regions of the hair plate throughout development (Fig. 2-7B, Table 2-2). The expansion in inter-sensilla space was relatively smaller than the overall enlargement of the hair plate surface area with maturation. For example, the pedicel increased in length by up to fivefold from N1 instar to adult (mean length: 113.0 ± 3.0 μm in N1, 591.3 ± 23.6 μm in adults), and the scape showed an even greater expansion of eightfold (mean length: 140.2 ± 4.5 μm in N1, 1172.3 ± 78.1 μm in adults). In contrast, the distance

between nearest sensilla increased by about 2.5-fold (mean distance: 25.1 ± 0.5 μm for the dorsal hair plate, 23.0 ± 0.8 μm for the lateral hair plate, respectively). The increasing rate of inter-sensilla distance was nearly comparable among the dorsal, ventral, medial, and lateral hair plates, indicating that they continued to share the same spatial scale during development.

Although new sensilla were added locally during development, the overall spacing between them still increased. These findings suggest that the addition of sensilla partially compensates for the reduction in spatial resolution caused by segmental growth. The number of sensilla increased progressively throughout development for all four locations of the hair plate. The dorsal hair plate in particular had more sensilla than the others, and this difference increased as the developmental stage progressed (Fig. 2-8: The number of sensilla in adults was 97.0 ± 3.8 μm for the dorsal, 25.0 ± 0.6 μm for the ventral, 23.3 ± 0.7 μm for the medial, and 24.7 ± 1.8 μm for the lateral hair plates, respectively). Alongside the increase in sensilla counts, the hair length of individual sensilla also elongated and became varied as the cricket developed (Fig. 2-9). The dorsal hair plate sensilla showed the greatest variation in their length. Even as the hair length became more varied, shorter sensilla remained to account for the majority across the developmental stages. This result suggests that the hair sensilla from the previous stage are replaced by elongated ones, with new, short sensilla added simultaneously during molting. These

developmental changes in the existing areas, number, and external morphology of the antennal hair plates are possibly involved in maintaining and refining their proprioceptive function in the active sensing of the antennae.

Multidimensional spatial analysis of hair plate sensilla across development

To quantitatively assess the consistency of hair plate spatial organization throughout development, I compared the distribution patterns of individual sensilla across samples and developmental stages using the Hausdorff distance of their three-dimensional coordinates (see Methods). This metric, indicating the maximum spatial deviation between the nearest two sensillar sensilla, can be used as a measure of geometric dissimilarity. I analyzed this metric separately for the dorsal, ventral, medial, and lateral hair plates and visualized pairwise distances between samples at the same and different developmental stages, as a heatmap (Fig. 2-10).

The Hausdorff distances for all four hair plates were smaller between samples at the same developmental stage than those at different stages, suggesting that the distribution pattern of hair plate sensilla was maintained reproducibly across individuals. Regarding the inter-stage variabilities among the four hair plates, the dorsal plate showed the smallest distances, indicating that the spatial arrangement of sensilla was consistent, especially in the dorsal plate throughout development. The sensillar distributions aligned

by the PCA method revealed that the number of sensilla increased by adding new sensilla to fill gaps between those existing at the previous stage (Figs. 2-3, 2-4, 2-5, 2-6). In addition, the length of individual sensilla on the hair plate correlated with their position within the hair array, with longer sensilla located distally than proximally. Furthermore, on the dorsal hair plate, hair length increased from the medial toward the lateral sides (Fig. 2-3). These overall spatial patterns of sensilla remained largely unchanged throughout developmental stages, without displacement or clustering shifts. Together, these results demonstrated that the spatial architecture of the hair plate system was highly conserved throughout development. The particularly low variation in the dorsal hair plate suggests that its spatial sensillar layout was tightly regulated. This possibly reflects its role in monitoring vertical antennal movements. These spatial organizations likely ensure consistent proprioceptive feedback during active sensing as the cricket grows.

2.4 Discussion

Developmental stability of spatial organization

In this chapter, I systematically mapped the three-dimensional morphology and spatial distribution of hair plate sensilla from the first instar to adulthood (Fig. 2-2). My results revealed that the spatial arrangements of hair plate sensilla were highly consistent across individuals throughout developmental stages, indicating a genetically determined organizational pattern. As the cricket developed, existing sensilla became more widely spaced, and new sensilla were added in specific regions, such as between longitudinal rows, along the peripheral margins, or near the base. This non-uniform but structured enlargement preserved the overall arrangement, maintaining the original spatial organization. This conserved organization likely ensures stable proprioceptive inputs even as the animal grows and its antennae elongate. This conserved arrangement of sensory organs may be controlled genetically, as demonstrated for the patterning of mechanosensory bristles in *Drosophila*, where the arrangement of epidermal sensory organs is regulated by genes such as hairy and by self-organized Notch signaling dynamics (Orenic et al., 1993; Corson et al., 2017).

Functional role of length and positional gradients

Interestingly, sensilla of distinct lengths were consistently located at corresponding relative positions in the antennal base segment across individuals and developmental stages. This conserved distribution pattern related to hair length suggests that the spatial organization of hair plate sensilla is tightly regulated during development. Such consistency is likely required for their function as proprioceptors, which accurately encode self-generated antennal movements based on the geometric structure of the antennal base. The number of hair plate sensilla in *G. bimaculatus* exceeds that reported in *Acheta domesticus* (dorsal: 52, ventral: 17, medial and lateral: 15) (McCarter and Loudon, 2025). This difference is likely due to its larger body size. However, it is also possible that ecological or behavioral differences between these species may influence receptor density. Species that depend more heavily on tactile exploration during locomotion likely require greater proprioceptive resolution, which could favor increased sensillar densities in specific hair plates. The larger number of sensilla in the dorsal hair plate also suggests its potential importance in detecting vertical orientation, which may be crucial for interpreting tactile contacts in relation to obstacle height and position during forward locomotion. Other insect mechanosensory systems, such as the filiform hair sensilla on the cricket cerci, serve as exteroceptive organs to detect unpredictable mechanical stimuli like air currents. These exteroceptive systems contain large numbers

of receptors distributed across broad surfaces (Shimozawa and Kanou, 1984). As shown in quantitative studies on the cercal sensory system, although interindividual variability in the number and placement of hair sensilla is relatively greater, the overall sensillar distribution on the cerci is organized based on their preferred direction of airflow stimuli, which is well approximated by computational models (Miller et al., 2011; Heys et al., 2012). This organized pattern of hair array is thought to enable robust detection by reducing noise through the high density of receptors. In contrast, the antennal hair plate system had fewer sensilla, which were more spatially restricted and aligned precisely. The consistent spatial pattern observed in all developmental stages likely reflects the proprioceptive roles of these receptors, which require providing reliable and steady inputs throughout postembryonic growth.

Consistent hair plate arrangements may support stable proprioceptive feedback for active sensing

The hair plates maintained nearly identical structures throughout development, which may guarantee the proprioceptive inputs essential for antennal mechanosensing. During tactile exploration, the animal must monitor the position of its antennae in real time. If the positions of sensilla varied with growth, proprioceptive feedback would be unreliable. The developmental stability in the spatial arrangement of hair plates reported

in this chapter suggests consistent population encoding of the antennal orientation across stages. This stable peripheral structure likely underlies the central neural processing of hair plate sensory inputs. In the next chapter, I investigated the central projections of sensory afferents from hair plates within the brain and suboesophageal ganglion to test whether the hair plate afferents form a topographic map like the cercal sensory system (Jacobs and Theunissen, 1996; Paydar et al., 1999).

2.5 Figures

(Figure 2-1)

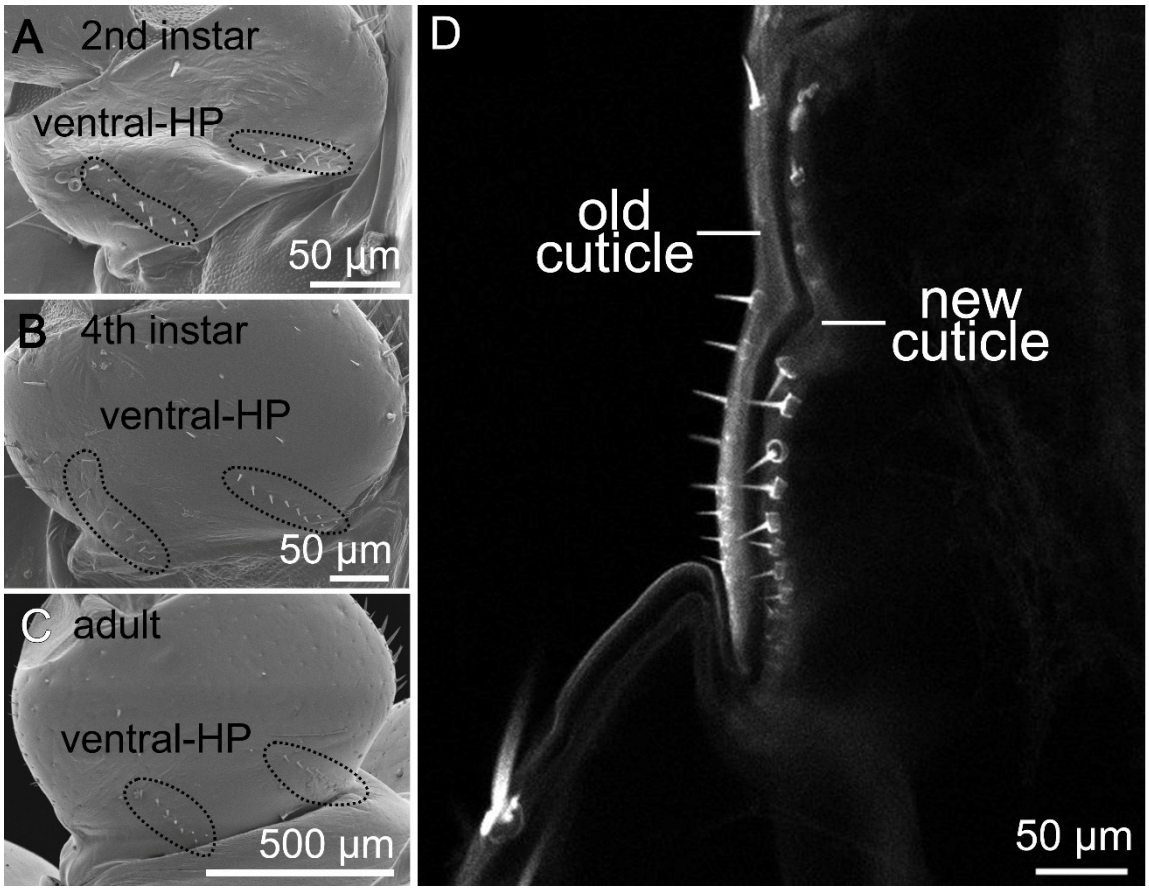

Figure 2-1. Developmental changes in the antennal base.

(A–C) Scanning electron micrographs of the ventral hair plate (ventral-HP) viewed from the ventral side of the scape in the (A) second instar, (B) fourth instar, and (C) adult. The areas enclosed by dotted lines indicate the e ventral-HP. **(D)** A confocal image of the antenna during molting from the final nymphal stage (N8) to adulthood.

(Figure 2-2)

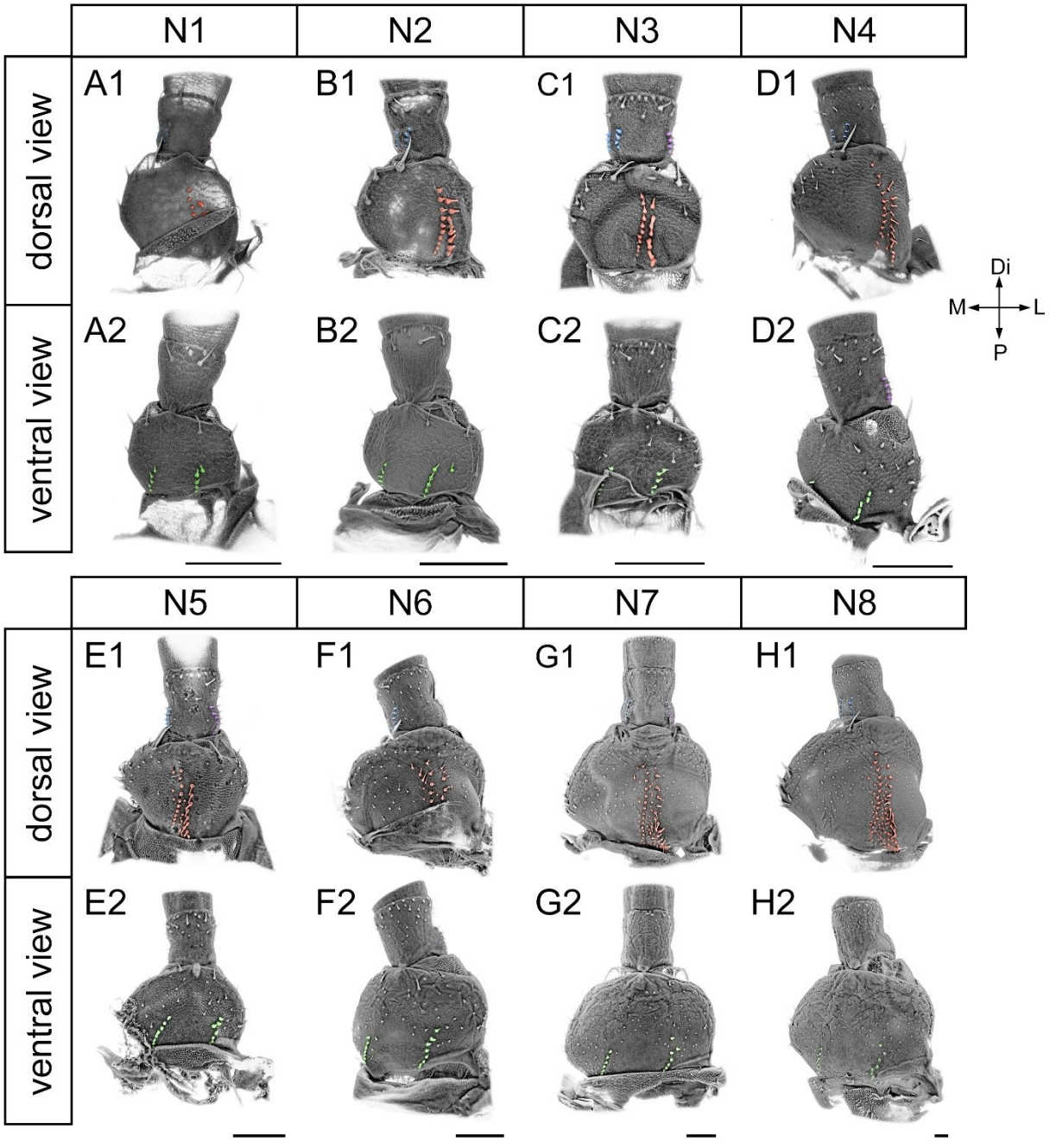

Figure 2-2. Three-dimensionally reconstructed antennal base and spatial distribution of hair plates across developmental nymphal stages.

(A–H) Dorsal **(A1–H1)** and ventral **(A2–H2)** views of the antennal base at different nymphal stages, N1 to N8. Sensilla of the medial, lateral, dorsal, and ventral hair plates (HP) hair plates were colored in cyan, purple, orange, and green, respectively. Di, distal; P, proximal; M, medial; L, lateral. Scale bars: 100 μm.

(Figure 2-3)

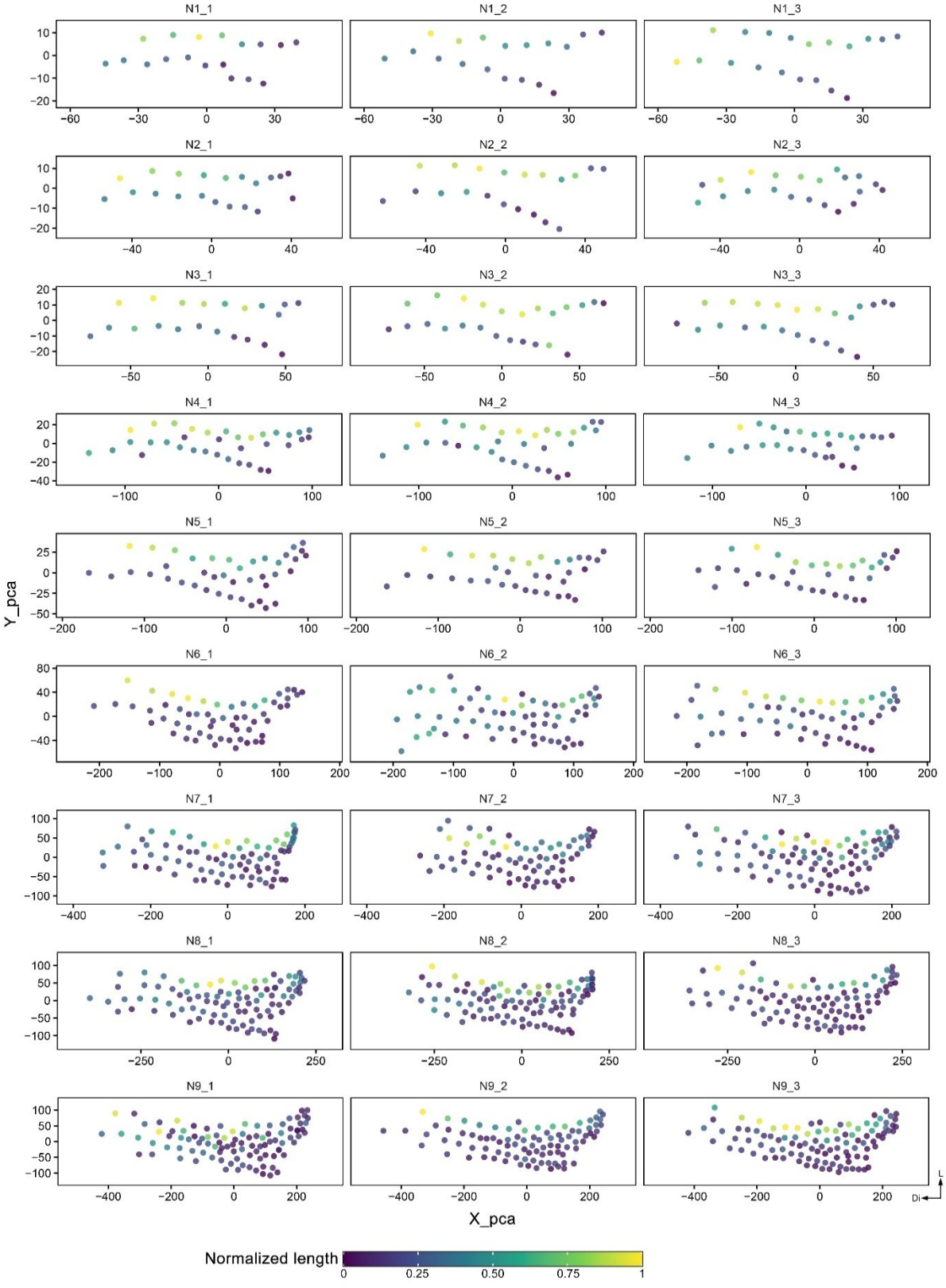
N1_1
N1_2
N1_3
N2_1
N2_2
N2_3
N3_1
N3_2
N3_3
N4_1
N4_2
N4_3
N5_1
N5_2
N5_3
N6_1
N6_2
N6_3
N7_1
N7_2
N7_3
N8_1
N8_2
N8_3
N9_1
N9_2
N9_3
Y_pca
X_pca
Normalized length
0
0.25
0.50
0.75
1

Figure 2-3. Standardized spatial distributions of dorsal hair plate sensilla across developmental stages.

Each dot represents an individual sensillum for the dorsal hair plate of the antennal base, plotted in the standardized XY-plane after principal component analysis (PCA) alignment (See Material and Methods). The data were obtained from 3 different samples for each developmental stage. Colors of dots indicate the normalized length.

(Figure 2-4)

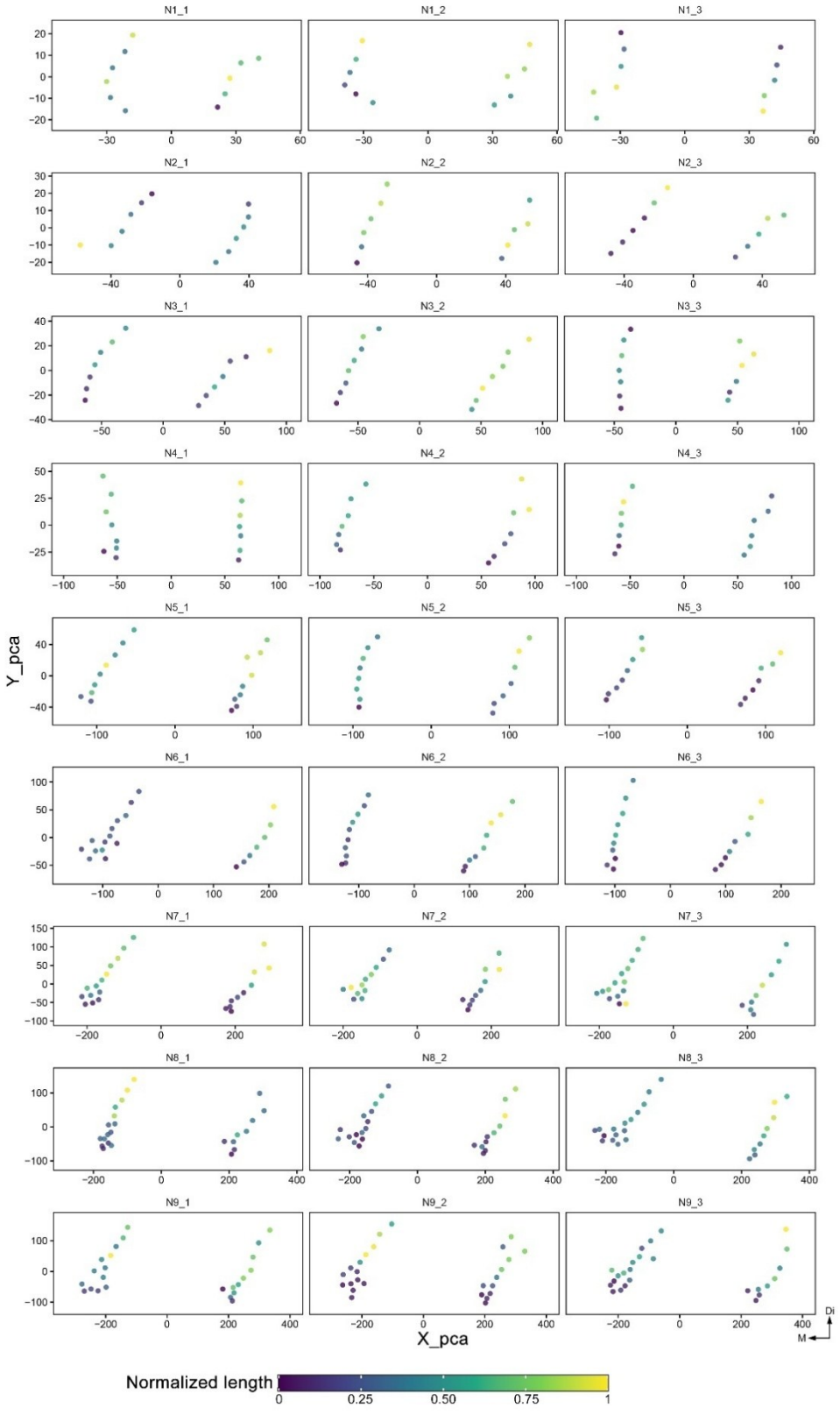
N1_1
N1_2
N1_3
N2_1
N2_2
N2_3
N3_1
N3_2
N3_3
N4_1
N4_2
N4_3
N5_1
N5_2
N5_3
N6_1
N6_2
N6_3
N7_1
N7_2
N7_3
N8_1
N8_2
N8_3
N9_1
N9_2
N9_3
Y_pca
X_pca
Normalized length
0
0.25
0.50
0.75
1

Figure 2-4. Standardized spatial distributions of ventral hair plate sensilla across developmental stages.

Each dot represents an individual sensillum for the ventral hair plate of the antennal base, plotted in the standardized XY-plane after principal component analysis (PCA) alignment(See Material and Methods). The data were obtained from 3 different samples for each developmental stage. Colors of dots indicate the normalized length..

(Figure 2-5)

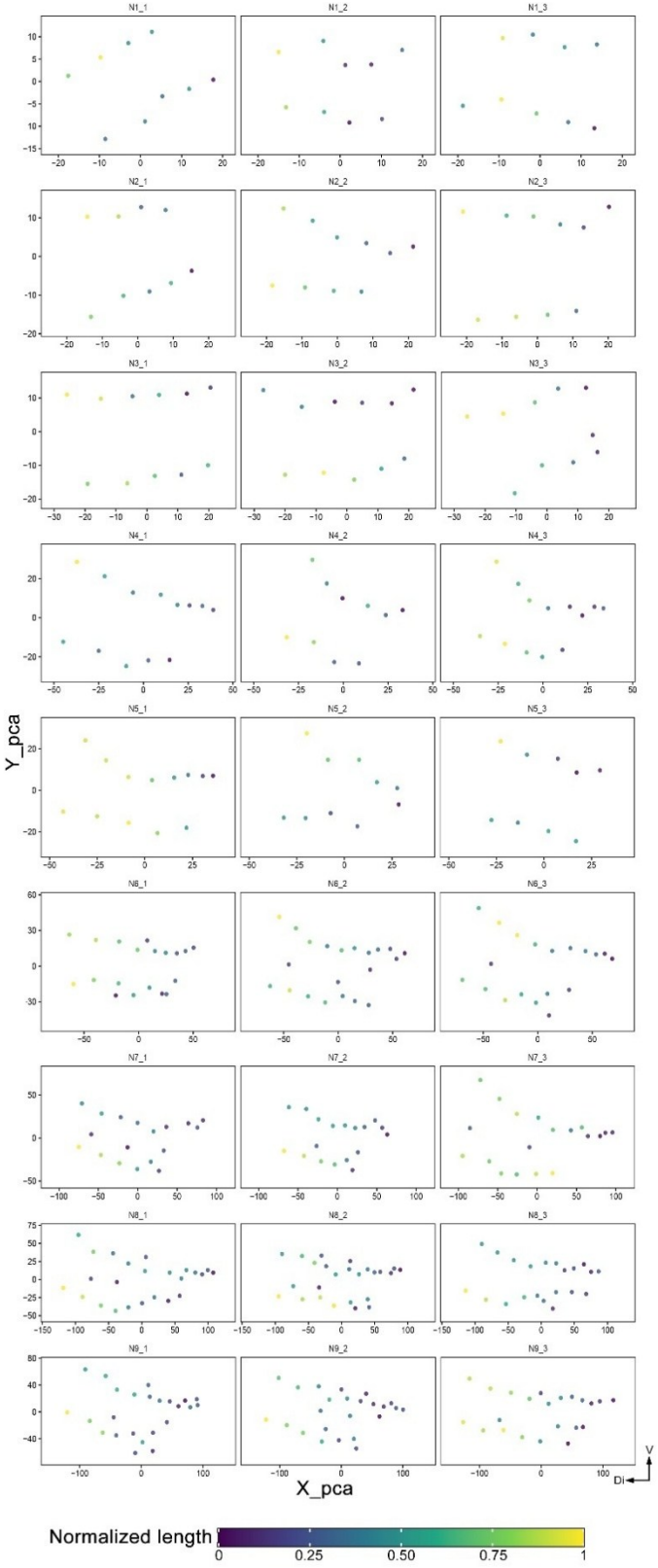
N1_1
N1_2
N1_3
N2_1
N2_2
N2_3
N3_1
N3_2
N3_3
N4_1
N4_2
N4_3
N5_1
N5_2
N5_3
N6_1
N6_2
N6_3
N7_1
N7_2
N7_3
N8_1
N8_2
N8_3
N9_1
N9_2
N9_3
Y_pca
X_pca
V
DI
Normalized length
0
0.25
0.50
0.75
1

Figure 2-5. Standardized spatial distributions of medial hair plate sensilla across developmental stages.

Each dot represents an individual sensillum for the medial hair plate of the antennal base, plotted in the standardized XY-plane after principal component analysis (PCA) alignment (See Material and Methods). The data were obtained from 3 different samples for each developmental stage. Colors of dots indicate the normalized length.

(Figure 2-6)

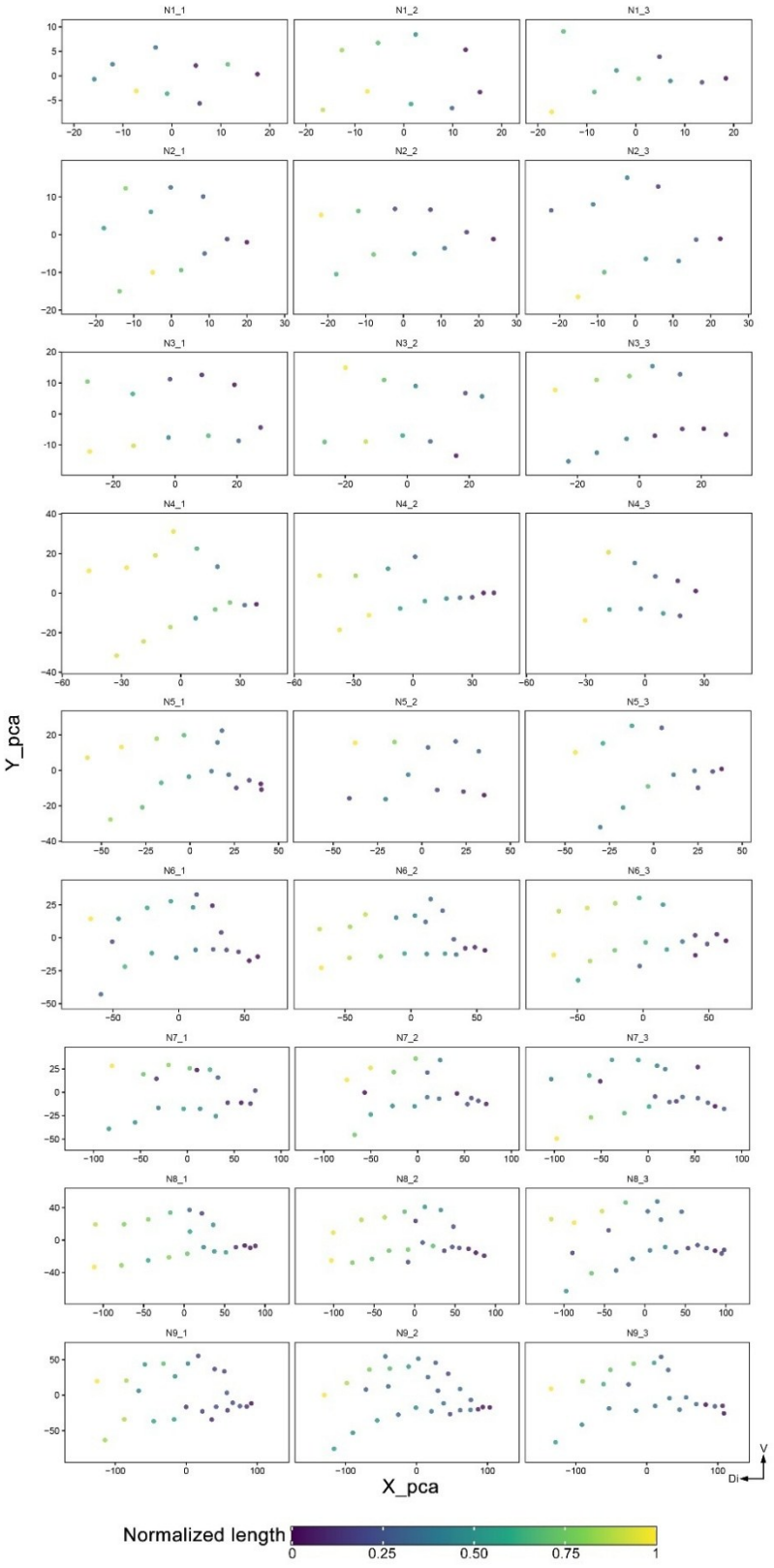
N1_1
N1_2
N1_3
N2_1
N2_2
N2_3
N3_1
N3_2
N3_3
N4_1
N4_2
N4_3
N5_1
N5_2
N5_3
N6_1
N6_2
N6_3
N7_1
N7_2
N7_3
N8_1
N8_2
N8_3
N9_1
N9_2
N9_3
Y_pca
X_pca
V
Di
Normalized length
0
0.25
0.50
0.75
1

Figure 2-6. Standardized spatial distributions of lateral hair plate sensilla across developmental stages.

Each dot represents an individual sensillum for the lateral hair plate of the antennal base, plotted in the standardized XY-plane after principal component analysis (PCA) alignment (See Material and Methods). The data were obtained from 3 different samples for each developmental stage. Colors of dots indicate the normalized length.

(Figure 2-7)

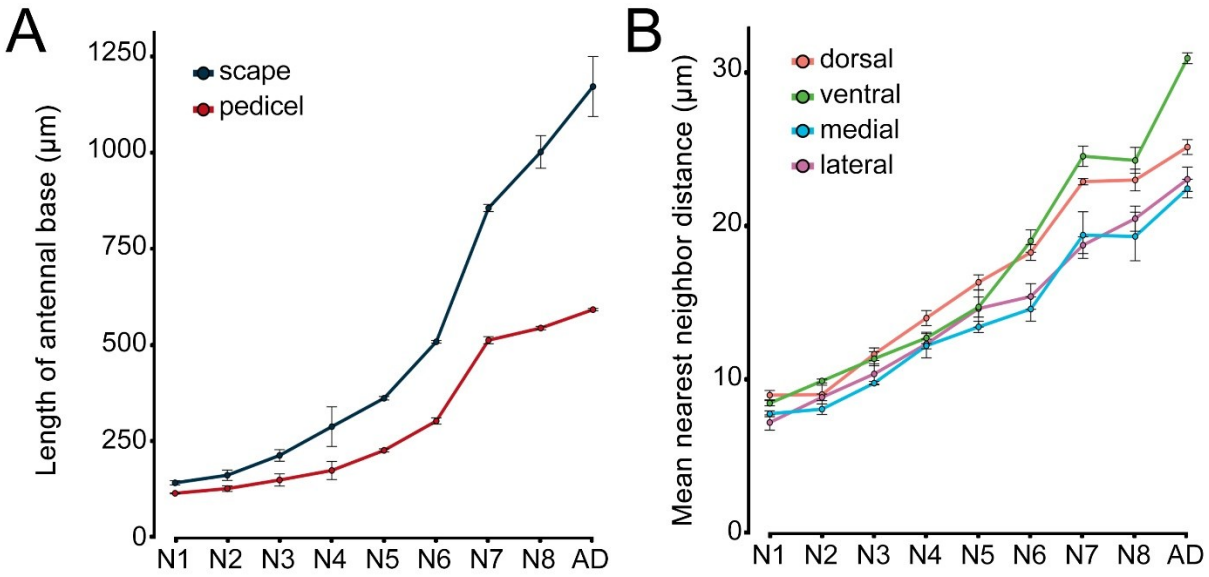

Figure 2-7. Developmental changes in antennal basal segments and hair plate sensilla distribution.

(A, B) Developmental curves of the antennal base segments (scape and pedicel, A) and hair plates (B) across developmental stages (N1–N8, AD: adult). The values for the vertical axis in **A** and **B** indicate the mean of the proximal-to-distal length of base segments (A) and the mean distance between the nearest sensilla within different locations of hair plates (B), respectively. Error bars indicate ± SEM.

(Figure 2-8)

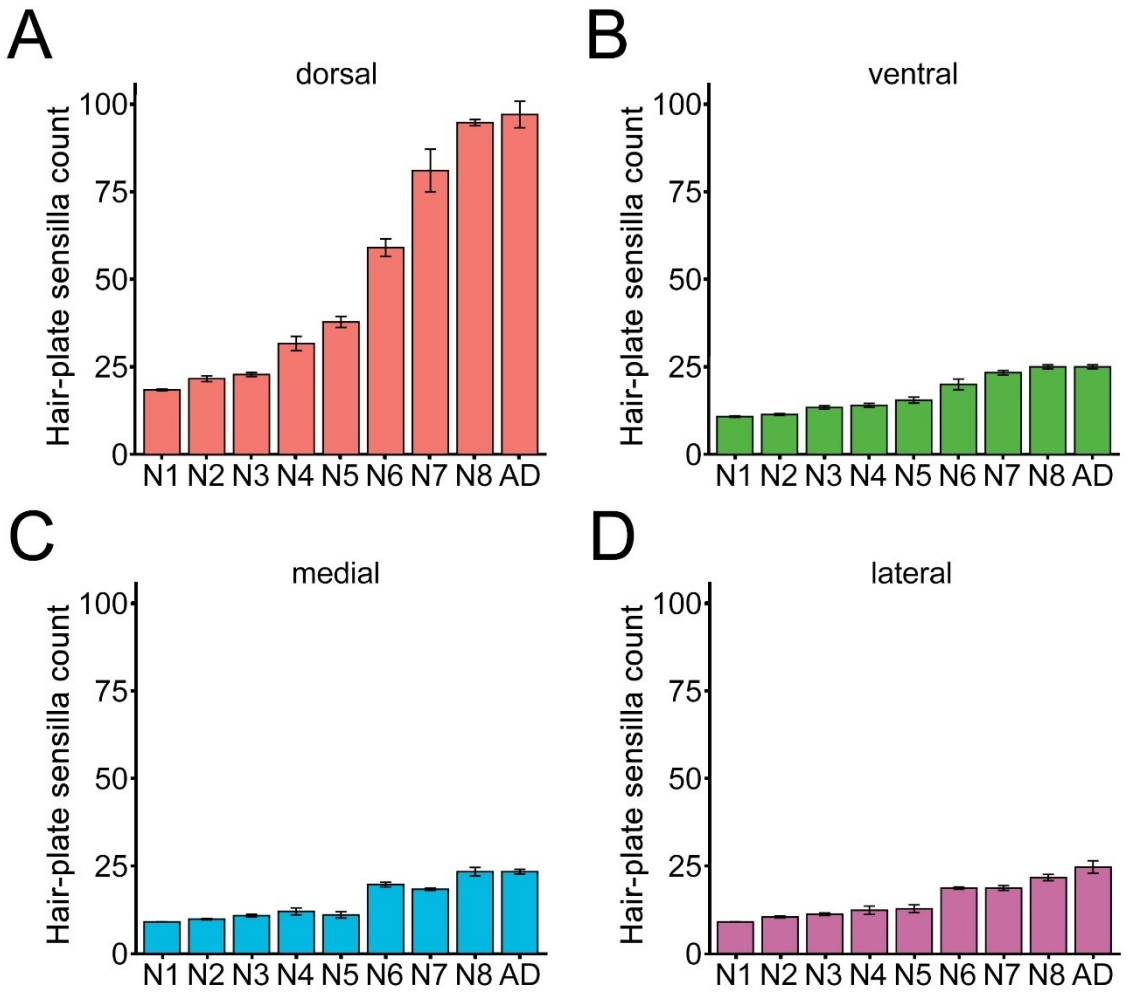

Figure 2-8. Developmental changes in the number of hair plate sensilla.

(A–D) Mean number of sensilla for the dorsal **(A)**, ventral **(B)**, medial **(C)**, and lateral **(D)** hair plates across developmental stages (N1–N8, AD: adult). Error bars indicate ± SEM.

(Figure 2-9)

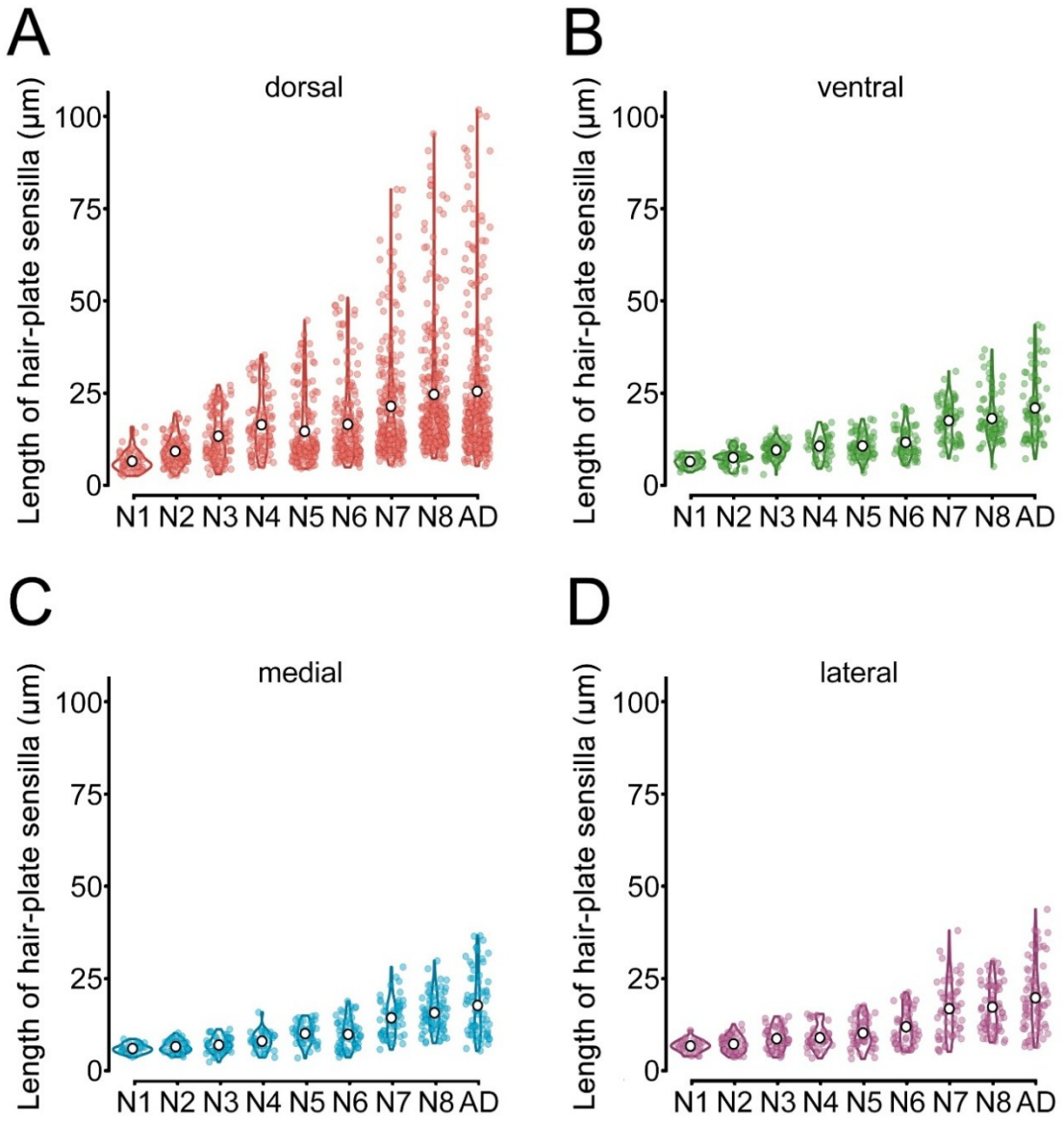

Figure 2-9 Developmental changes in the length of individual hair plate sensilla.

(A–D) The hair lengths of individual sensilla for the dorsal **(A)**, ventral **(B)**, medial **(C)**, and lateral **(D)** hair plates across developmental stages (N1–N8, AD: adult). Colored open circles represent data for each sensillum, and white filled circles indicate median values. Colored lines represent the distribution of the hair length.

(Figure 2-10)

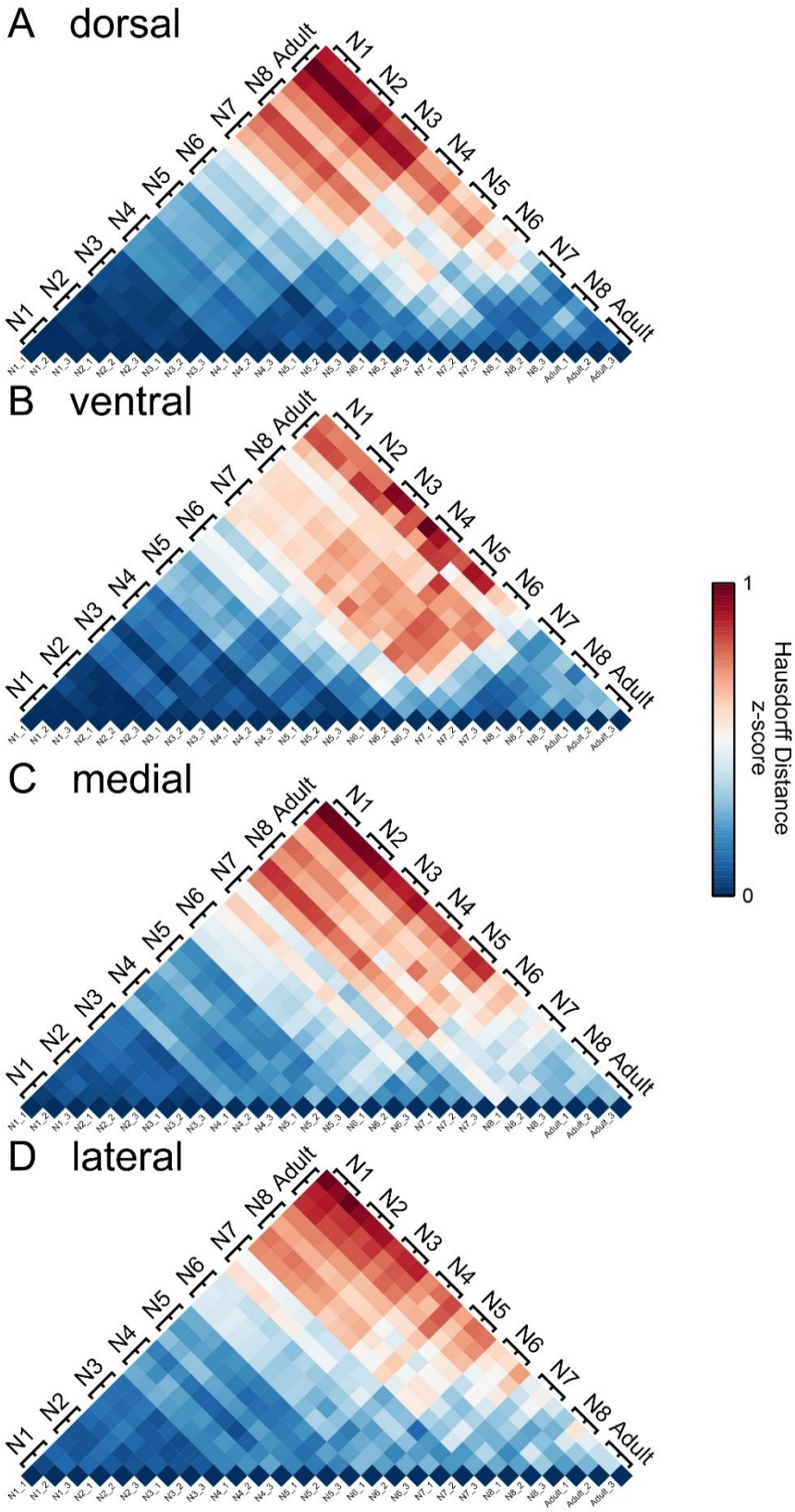
A dorsal
B ventral
C medial
D lateral
N1
N2
N3
N4
N5
N6
N7
N8
Adult
1
0
Hausdorff Distance
z-score

Figure 2-10. Similarity in spatial arrangement of hair plate sensilla across developmental stages.

(A–D) Heatmaps depicting pairwise spatial similarity in the spatial distribution of hair plate sensilla among samples for four different locations: dorsal (A), ventral (B), medial (C), and lateral (D). Each cell in the heatmap represents a pairwise comparison between two individual specimens. The colors for each matrix entry represent the normalized Hausdorff distance (z-score) between two samples calculated from the three-dimensional arrangement of the hair plate sensilla. As shown in the color table on the right, blue represents a shorter distance, indicating greater spatial similarity, while red represents a longer distance, indicating lower similarity.

2.6 Tables

(Table 2-1)

Table 2-1. Developmental change in scape and pedicel length data for Fig. 2-7A.

Stage	Segment	Segment length (μm, mean ± SEM)	Sample size
N1	Scape	143.00 ± 7.57	3
	Pedicel	111.67 ± 5.24	3
N2	Scape	162.33 ± 9.21	3
	Pedicel	123.67 ± 6.96	3
N3	Scape	207.33 ± 3.71	3
	Pedicel	147.33 ± 1.33	3
N4	Scape	297.00 ± 11.79	3
	Pedicel	177.00 ± 9.71	3
N5	Scape	361.00 ± 13.45	3
	Pedicel	225.33 ± 10.53	3
N6	Scape	484.67 ± 9.77	3
	Pedicel	286.00 ± 1.53	3
N7	Scape	856.00 ± 42.50	3
	Pedicel	511.67 ± 15.90	3
N8	Scape	1002.00 ± 51.64	3
	Pedicel	543.33 ± 4.37	3
Adult	Scape	1251.67 ± 81.67	3

	Pedicel	628.00 ± 18.34	3

(Table 2-2)

Table 2-2. Mean nearest-neighbor distances data for Fig. 2-7B.

Stage	Hair plate	Nearest-neighbor distance (μm, mean ± SEM)	Sample size
N1	Dorsal	8.98 ± 0.30	3
	Lateral	7.20 ± 0.50	3
	Medial	7.76 ± 0.19	3
	Ventral	8.45 ± 0.17	3
N2	Dorsal	9.02 ± 0.61	3
	Lateral	8.84 ± 0.22	3
	Medial	8.07 ± 0.34	3
	Ventral	9.90 ± 0.12	3
N3	Dorsal	11.64 ± 0.41	3
	Lateral	10.36 ± 0.67	3
	Medial	9.76 ± 0.11	3
	Ventral	11.35 ± 0.46	3
N4	Dorsal	14.00 ± 0.49	3
	Lateral	12.31 ± 0.31	3
	Medial	12.19 ± 0.79	3
	Ventral	12.70 ± 0.37	3
N5	Dorsal	16.33 ± 0.49	3
	Lateral	14.62 ± 1.21	3
	Medial	13.42 ± 0.37	3
	Ventral	14.71 ± 0.65	3
N6	Dorsal	18.27 ± 0.51	3
	Lateral	15.40 ± 0.84	3
	Medial	14.59 ± 0.79	3

	Ventral	19.02 ± 0.73	3
N7	Dorsal	22.88 ± 0.20	3
	Lateral	18.75 ± 0.54	3
	Medial	19.40 ± 1.52	3
	Ventral	24.54 ± 0.66	3
N8	Dorsal	22.99 ± 0.71	3
	Lateral	20.48 ± 0.82	3
	Medial	19.32 ± 1.58	3
	Ventral	24.27 ± 0.85	3
Adult	Dorsal	25.14 ± 0.48	3
	Lateral	23.04 ± 0.79	3
	Medial	22.43 ± 0.61	3
	Ventral	30.92 ± 0.35	3

Chapter 3: Central projection of antennal mechanosensory afferents

3.1 Introduction

Antennal mechanosensation plays a key role in guiding insect behavior, especially during active tactile exploration (Harley et al., 2009; Krause and Dürr, 2012). My research in the previous chapters indicated that hair plates at the antennal joints are located at suitable positions to provide proprioceptive signals about joint angles and flagellum movements. These signals would allow insects to monitor their antennal trajectory during active scanning and serve as a reference for identifying spatial information about contacted objects, such as their location, distance, and shape, through active tactile sensing. Tactile stimulation of the antennae elicits various behaviors, such as walking (Okada and Toh, 2001, 2006) and running (Camhi and Johnson, 1999; Cowan et al., 2006; Mongeau et al., 2013, 2015). In these behavioral studies, it has been revealed that antennal position strongly influences action selection in insects. However, although behavioral and anatomical studies have suggested the involvement of central processing of antennal inputs, the detailed organization of the central pathways and the processing of hair plate signals are still not fully elucidated.

Anatomical and imaging studies have demonstrated that sensory afferents from flagellar mechanoreceptors exhibit somatotopic organization within the deutocerebrum and subesophageal ganglion in cockroaches and crickets (Nishino et al., 2005; Bayley and Hedwig, 2018). The filiform hair sensilla on the cerci, which are abdominal mechanosensory organs, also form a precise neural map where airflow direction is represented in the spatial arrangement of afferents (Jacobs and Theunissen, 1996; Paydar et al., 1999; Ogawa et al., 2006). These facts raise the possibility that the sensory afferent projections of antenna hair plates are also arranged topographically according to the antenna orientation. Clarifying the projection pathway and its terminal patterns is important for understanding how proprioceptive information about antennal orientation is produced. The hair plate afferent signals encoding each joint angle across different axes would need to be integrated to represent 3D antennal movements.

In contrast, few studies have examined the sensory responses of the hair plate to antennal movements in insects. Previous work showed that single hair plate receptors generate phasic–tonic spikes suitable for detecting joint position (Okada and Toh, 2001). Ache and Dürr (2015) proposed a model predicting how mechanosensory inputs could be combined across many receptors in stick insects, but this prediction remained theoretical. However, these studies either focused on single sensilla or relied on computational estimates of population coding. To date, no electrophysiological study has directly

measured the ensemble activity of hair plate afferents in three-dimensional space. Electrophysiological studies in descending interneurons have revealed that they encode the velocity of antennal movements in a specific direction (Gebhardt and Honegger, 2001). However, neural signals encoding antennal angle and direction at the moment, which are provided by hair plate inputs, would be necessary for active sensing. Thus, understanding how interneurons linking mechanosensory afferents and descending neurons encode the direction and magnitude of antennal movement is also crucial for exploring the neural basis of antennal active sensing.

In this chapter, I examined how hair plate afferents project into the central nervous system. I identified the projection patterns of their axons and described how these sensory fibers enter and branch within the brain. I also used retrograde staining to reveal the central projections of hair plate sensilla. These results provide a clear anatomical framework for understanding how antennal movements are represented in the brain and offer a basis for future studies on sensorimotor integration in insects.

3.2 Materials and Methods

The materials and methods used in the *Animals* section were identical to those in Chapter 1.

Anterograde staining of sensory afferents

Adult male crickets were used for anterograde staining. Crickets were anesthetized on crushed ice to prevent their movements. After cutting the sensilla of one or two hair plates on the scape or pedicel with a razor blade, a glass micropipette filled with a dye solution containing 1% Alexa Fluor 488 or 1% Alexa Fluor 594 dextran conjugates (10,000 MW; Thermo Fisher Scientific) diluted in distilled water was placed in contact with the cut area. To perform double staining of multiple hair plates, two micropipettes, each filled separately with Alexa Fluor 488 or 594, were placed in contact with different target regions. The glass pipettes were secured with clay, and the specimens were kept in a moist chamber at 4 ℃ overnight. The cephalic ganglia, including the brain, suboesophageal ganglion (SOG), and ventral nerve cords connecting them, were then isolated, transferred onto filter paper for shaping, and fixed with 4% paraformaldehyde (PFA) for 6 hours. After fixation, the ganglia were dehydrated in an ascending ethanol series (50%, 70%, 90%, and 100%; 5 min each) and then cleared in methyl salicylate.

Confocal imaging of sensory afferents

The stained mechanosensory afferents of the hair plates were imaged using a confocal laser scanning microscope (LSM980, Zeiss) equipped with a 10× dry objective (Plan-Apochromat 10×/0.45 M27, Zeiss). Optical sectioned images with a resolution of 1024 × 1024 pixels (pixel size 0.83 μm × 0.83 μm) were captured at 1 μm Z-steps from the ventral to dorsal side of the ganglion. Using *ImageJ* (version 1.54), the Z-stack series of images was merged into a single image and adjusted for brightness and contrast to clearly visualize the full morphology of the afferents.

3.3 Results

Central projection of hair plate afferents

Anterograde labeling of the sensory afferents also visualized the cell bodies at the base of the antenna, where the axons originated from spatially dispersed cell bodies and converged into distinct axon bundles (Fig. 3-1A). This bundle then travelled through the antennal nerve and reached the lateral region of the dorsal lobe (DL) in the brain. Within the DL, these axons branched to collaterals (Fig. 3-1B). After branching, their axon, referred to as T6-1, further descended to the ipsilateral region of the subesophageal ganglion (SOG). The major axon collaterals, T6-2, ran dorso-medially and terminated in the dorso-medial region of the DL, which corresponds to the antennal mechanosensory and motor center (AMMC; Yoritsune and Aonuma, 2012). In addition, the axon had small terminal branches, T6-3, in the dorso-lateral area of AMMC (LAMMC), before branching to T6-1 and T6-2. The sensory afferents, including collaterals, terminated within the ipsilateral hemisphere of the ganglia and never extended across the midline. The projected regions of hair plate afferents in DL did not extend to the ventral flagellum area (VFA; Fig. 3-1B) suggesting that they are anatomically segregated from the flagellar mechanoreceptor pathways and serve distinct functions. Hair plates likely convey proprioceptive information about antennal joint angles rather than mechanosensory input from the flagellum. This projection pattern was consistent across all anatomical positions

of the hair plates, indicating that the afferent organization was not position-specific but shared among dorsal, ventral, medial, and lateral hair plates (Fig. 3-2A–D). Although afferent fibers from the dorsal, ventral, medial, and lateral hair plates entered the AMMC through partially segregated routes, their axonal trajectories overlapped substantially between the AMMC and SOG.

Overlapping projection patterns without topographic segregation

To compare the projection patterns of sensory afferents from hair plates at different locations, I performed dual anterograde labeling with two different fluorophores (See Methods, Fig. 3-2). Their axons entered the deutocerebrum from slightly different routes depending on the hair plate of origin. However, the trajectories of these afferents converged just after entering the DL, and their terminal fields substantially overlapped. This overlap was observed across all combinations of dorsal, ventral, medial, and lateral hair plates. No clear spatial segregation, suggestive topographic map, was observed. This result suggests that positional information about the antennal movement axis from the periphery is not spatially represented in the processing center but rather decoded by specific postsynaptic neurons, such as the labeled-line system.

3.4 Discussion

Integration pattern of hair plate projections in the central nervous system

Neural tracing experiments demonstrated that all hair plate afferents project to both the antennal mechanosensory and motor center (AMMC) and the subesophageal ganglion (SOG), without extending into the ventral flagellar afferent (VFA) region. This projection pattern closely parallels recent findings in the cockroach brain, where dye filling of the scapus-pedicel joint revealed dense innervation of both the medial and lateral subregions of the AMMC, but not the VFA (Althaus et al., 2022). Functional imaging studies have shown that different mechanosensory modalities drive calcium increases in distinct dendritic regions and that touch of the flagellum is represented as a topographic map along the dendritic tree of target neurons (Bayley and Hedwig, 2018). Consistent with this, anatomical studies in cockroaches demonstrated that tactile afferents from the antenna exhibit somatotopic organization, with neurons located more distally in the flagellum projecting to progressively more medioventral regions in the deutocerebrum and subesophageal ganglion (Nishino et al., 2005). In contrast, although projections from different hair plates exhibited partially distinct collateral patterns, my experiments showed no evidence of a clear topographic map within the AMMC or SOG (Fig. 3-2). However, it should be noted that the anterograde tracing used here may not have labeled all sensory neurons, leaving the possibility that a few afferents were missed and that fine-

scale variations went undetected. These findings suggest that positional information from antennal hair plates is centrally integrated rather than mapped in a one-to-one spatial fashion, as observed for flagellar input. This supports the view that the AMMC functions as an integrative hub for multiple mechanosensory streams, with the organization and function of hair plate inputs distinct from those of flagellar afferents. In contrast, the cerci system provides an example of a true afferent map, where the directional sensitivity of giant interneurons (GIs) primarily depends on the relative positions of their dendrites within the spatial map formed by mechanosensory afferents (Jacobs and Theunissen, 2000; Ogawa and Mitani, 2015). Due to the considerable individual variability in the number of filiform hairs on the cerci, integration between afferent input and the dendritic architecture of GIs is necessary to achieve reliable spatial coding. In the antennal hair plate system, however, the spatial organization of the sensilla is already highly stereotyped and consistent across individuals. This precise arrangement at the level of the sensory receptors means that the direction and movement state of the antenna can be robustly transmitted to descending neurons and central circuits, even in the absence of a topographic map at higher-order processing levels. Thus, unlike the cerci system, the antennal hair plate pathway may rely less on central spatial mapping and more on the inherent organization and developmental precision of its input layer.

3.5 Figures

(Figure 3-1)

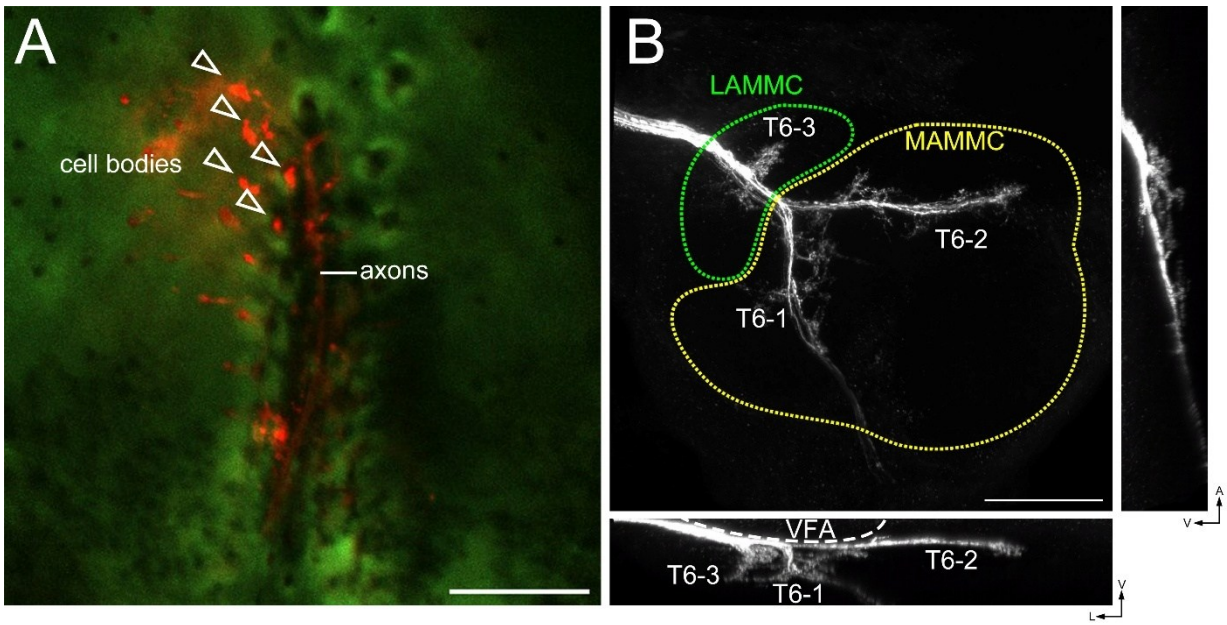

Figure 3-1. Central projections of mechanosensory afferents from hair plates.

(A) A confocal stack image showing peripheral branches of sensory afferents for the dorsal hair plate. Cell bodies are observed at the position close to the base of individual hair sockets, and their axons converge into a bundled projection. Sensory neurons are labeled in red, and cuticle autofluorescence is shown in green. Scale bars: 100 μm

(B) Fluorescent image of the deutocerebrum showing anterograde single labeling of sensory afferents from the dorsal hair plates. The projection terminals are distributed within the medial and lateral antennal mechanosensory and motor centers (MAMMC and LAMMC). A, anterior; V, ventral; L, lateral. Scale bars: 100 μm

(Figure 3-2)

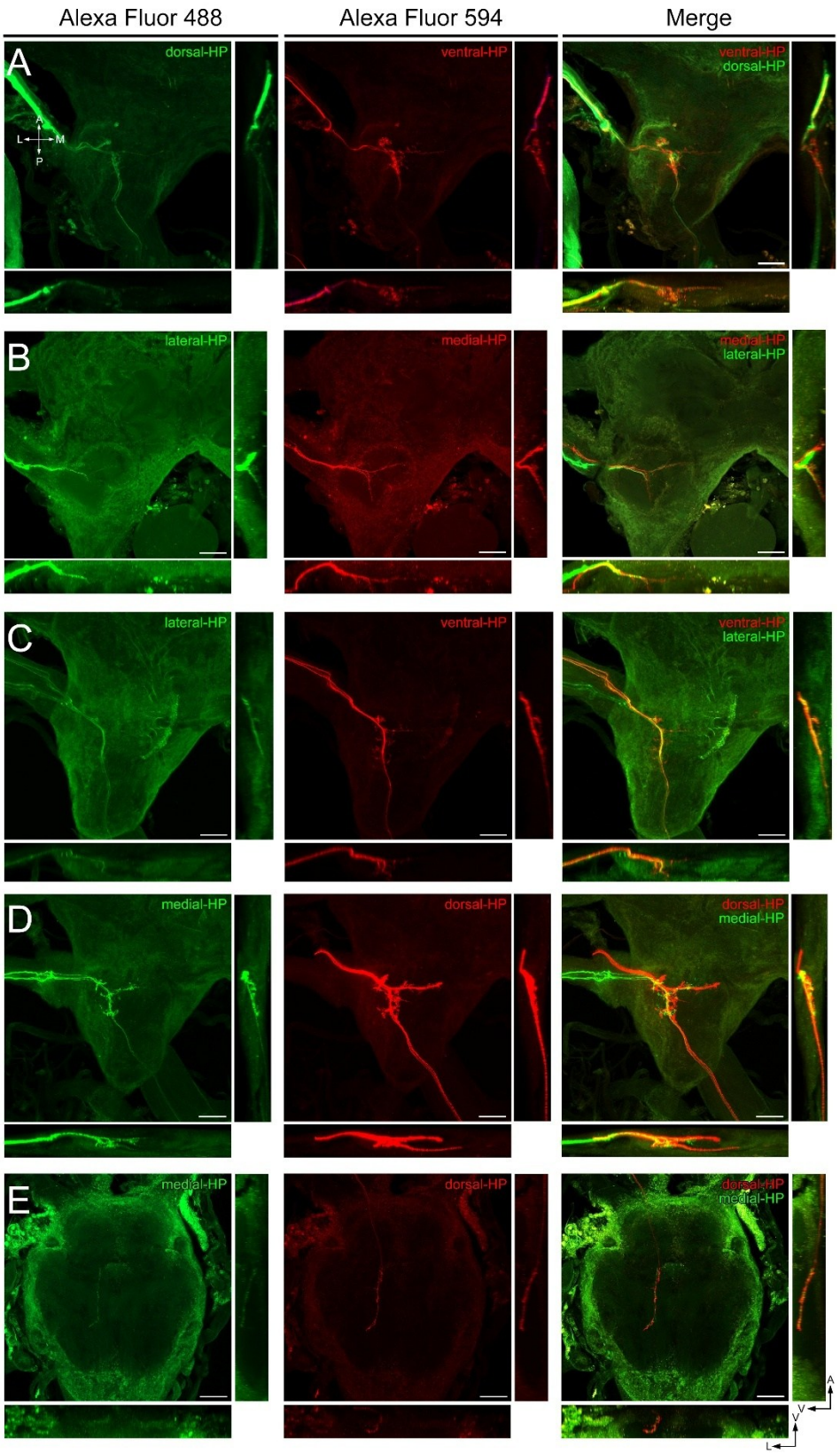
Alexa Fluor 488
Alexa Fluor 594
Merge
A
dorsal-HP
ventral-HP
ventral-HP
dorsal-HP
A
L
M
P
B
lateral-HP
medial-HP
medial-HP
lateral-HP
C
lateral-HP
ventral-HP
ventral-HP
lateral-HP
D
medial-HP
dorsal-HP
dorsal-HP
medial-HP
E
medial-HP
dorsal-HP
dorsal-HP
medial-HP
A
V
V
L

Figure 3-2. Central projections of mechanosensory afferents from hair plates.

(A–D) Fluorescent image of deutocerebrum showing anterograde double labeling of sensory afferents from the ventral and dorsal hair plates **(A)**, from the medial and lateral hair plates **(B)**, from the ventral and lateral hair plates **(C)**, and from dorsal and medial hair plates **(D)**. **(E)** Fluorescent image of SOG showing afferent projections from dorsal and medial hair plates. A, anterior; P, proximal; M, medial; L, lateral. Scale bars: 100 μm

General Discussion

Proprioceptive information provided by the antennal hair plates

Previous physiological studies have shown that scapal hair plate receptors of cockroaches exhibit phasic-tonic discharge in response to antenna deflection (Okada and Toh, 2001). The variety in sensillar morphology, including differences in length and orientation, likely enables the hair plate system to detect a broad range of antennal movement dynamics. The computational model of Ache and Dürr (2015) demonstrated that antennal movement gradually deflects individual sensilla, so that the greater the joint displacement, the more sensilla are activated in the hair plate. This suggests that both the activity of individual sensilla and the population signal reliably encode the joint angle correlated with antennal movements.

However, their model did not include variation in sensillar length. My morphological data revealed that the hair lengths varied depending on their position within the organized spatial pattern. Specifically, shorter hairs were typically located closer to the joint, where they could be activated by a smaller change in joint angle. In contrast, longer hairs positioned farther from the joint would respond to a greater displacement. This systematic distribution likely provides a functional architecture that enables continuous and fine-scale monitoring of antennal joint angles. Previous behavioral studies have clearly shown that crickets and cockroaches can perceive

antennal orientation with high accuracy (Okada and Toh, 2004; 2006; Ifere et al., 2022; 2025). Proprioceptive information about antennal orientation may be encoded through different mechanisms from the topographic map.

Functional significance of reafferent inputs for active sensing

Many species of insects, such as crickets and cockroaches, actively move their antennae to sense their surroundings. Thus, antennal mechanosensory signals can originate from either self-generated movements or passive contact with external objects. In this study, I found that antennal hair plates exhibit a joint-axis–aligned sensillar organization, a highly reproducible spatial arrangement across individuals and developmental stages, and selective afferent projections to antennal motor and sensorimotor integration centers. Based on these findings, antennal hair plates serve as key proprioceptors that encode antennal movement during active sensing (Ache and Dürr, 2015). Similar mechanisms have been observed in cockroaches, stick insects, and moths, suggesting a conserved role of antennal hair plates across insect species (Okada and Toh, 2004; Jaske et al., 2021; Krishnan et al., 2012). Owing to its robust anatomical organization and genetic consistency, the cricket serves as a powerful model for unraveling the principles of proprioceptive feedback and active sensing.

A recent theory frames active sensing as a closed-loop “sensory-energetic loop” (Ahissar and Assa, 2016). In this framework, alloactive sensing describes situations where an animal adjusts its sensors to detect the environment, whereas homeoactive sensing refers to cases where the animal alters its environment. In the tactile sensory system, both types of sensing often occur simultaneously; therefore, animals must predict the sensory consequences or reafferent inputs generated by their own actions (Zweifel and Hartmann, 2020). Unlike typical active sensing frameworks, however, reafferent inputs mediated by the activation of hair plates during active scanning of antennae do not alter the environment. In this context, rather than predicting sensory outcomes, it is necessary to monitor in real time which area of space the antenna is currently exploring. It is proposed that this information is provided by proprioceptive inputs from the hair plates, enabling spatial awareness through antennal exploration (Ifere et al., 2022; 2025).

The precise and reproducible spatial organization of hair plate sensilla allows the spatially structured recruitment of receptor activation, which may contribute to a reliable neural representation of antennal position. Future physiological studies on postsynaptic neurons downstream of the hair plates will clarify how antennal angles are decoded. In addition to these experiments, the computational model based on the morphometric data of hair plate sensilla, including their three-dimensional distribution and length reported

in this study, as well as antennal kinematics, will clarify how reafferent information is represented during active tactile exploration.

References

Ache JM, Dürr V (2015) A computational model of a descending mechanosensory pathway involved in active tactile sensing. PLoS Comput Biol 11:e1004263. https://doi.org/10.1371/journal.pcbi.1004263

Ahissar E, Assa E (2016) Perception as a closed-loop convergence process. eLife 5:e12830. https://doi.org/10.7554/eLife.12830

Allgäuer C, Honegger HW (1993) The antennal motor system of crickets: modulation of muscle contraction by a common inhibitor, DUM neurons, and proctolin. J Comp Physiol A 173:485–494. https://doi.org/10.1007/BF00193521

Alt H, Braß P, Godau M, Knauer C, Wenk C (2003). Computing the Hausdorff distance of geometric patterns and shapes. In: Aronov B, Basu S, Pach J, Sharir M (eds) Discrete and computational geometry. Algorithms and combinatorics, vol 25. Springer, Berlin, Heidelberg. https://doi.org/10.1007/978-3-642-55566-4_4

Althaus V, Jahn S, Massah A, Stengl M, Homberg U (2022) 3D atlas of the brain of the cockroach *Rhyparobia maderae*. J Comp Neurol 530:3126–3156. https://doi.org/10.1002/cne.25396

Baba Y, Comer CM (2008) Antennal motor system of the cockroach, *Periplaneta americana*. Cell Tissue Res 331:751–762. https://doi.org/10.1007/s00441-007-0545-9

Bayley TG, Hedwig B (2018) Dendritic Ca2+ dynamics and multimodal processing in a cricket antennal interneuron. J Neurophysiol 120:910–919. https://doi.org/10.1152/jn.00663.2017

Brézot P, Tauban D, Renou M (1996) Sense organs on the antennal flagellum of the green stink bug, *Nezara viridula* (L.) (Heteroptera: Pentatomidae): Sensillum types and numerical growth during the post-embryonic development. Int J Insect Morphol Embryol 25(4):427–441. https://doi.org/10.1016/S0020-7322(96)00012-8

Bush NE, Solla SA, Hartmann MJ (2016) Whisking mechanics and active sensing. Curr Opin Neurobiol 40:178–188. https://doi.org/10.1016/j.conb.2016.08.001

Camhi JM, Johnson EN (1999) High-frequency steering maneuvers mediated by tactile cues: antennal wall-following by the cockroach. J Exp Biol 202:631–643. https://doi.org/10.1242/jeb.202.5.631

Carle T, Yamawaki Y, Watanabe H, Yokohari F (2014) Antennal development in the praying mantis (*Tenodera aridifolia*) highlights multitudinous processes in hemimetabolous insect species. PLoS One 9:e98324. https://doi.org/10.1371/journal.pone.0098324

Chakrabarti S, Schwarz C (2018) Cortical modulation of sensory flow during active touch in the rat whisker system. Nat Commun 9:2630. https://doi.org/10.1038/s41467-018-06200-6

Chen S, Augustine GJ, Chadderton P (2016) The cerebellum linearly encodes whisker position during voluntary movement. eLife 5:e10509. https://doi.org/10.7554/eLife.10509

Chinta P, Pluta SR, et al. (2025) Whisking and locomotion are jointly represented in superior colliculus neurons. PLoS Biol 23:e3003087. https://doi.org/10.1371/journal.pbio.3003087

Comer C, Baba Y (2011) Active touch in orthopteroid insects: behaviours, multisensory substrates and evolution. Philos Trans R Soc B 366:3006–3015. https://doi.org/10.1098/rstb.2011.0149

Comer CM, Parks L, Halvorsen MB, Breese-Terteling A (2003) The antennal system and cockroach evasive behavior. II. Stimulus identification and localization are separable antennal functions. J Comp Physiol A 189:97–103. https://doi.org/10.1007/s00359-002-0384-9

Corson F, Couturier L, Rouault H, Mazouni K, Schweisguth F (2017) Self-organized Notch dynamics generate stereotyped sensory organ patterns in *Drosophila*. Science 356:eaai7407. https://doi.org/10.1126/science.aai7407

Cowan NJ, Lee J, Full RJ (2006) Task-level control of rapid wall following in the American cockroach. J Exp Biol 209:1617–1629. https://doi.org/10.1242/jeb.02166

Crapse TB, Sommer MA (2008) Corollary discharge across the animal kingdom. Nat Rev Neurosci 9:587–600. https://doi.org/10.1038/nrn2457

Ebert C, Bagdasarian K, Haidarliu S, Ahissar E, Wallach A (2021) Interactions of whisking and touch signals in the rat brainstem. J Neurosci 41:4826–4839. https://doi.org/10.1523/JNEUROSCI.1410-20.2021

Engelmann J, Pusch R, von der Emde G (2008) Active sensing. Commun Integr Biol 1:29–31. https://doi.org/10.4161/cib.1.1.6609

Gebhardt M, Honegger HW (2001) Physiological characterisation of antennal mechanosensory descending interneurons in an insect (*Gryllus bimaculatus*, *Gryllus campestris*) brain. J Exp Biol 204:2265–2275. https://doi.org/10.1242/jeb.204.13.2265

Gnatzy W (1978) Development of the filiform hairs on the cerci of *Gryllus bimaculatus* Deg. (Saltatoria, Gryllidae). Cell Tissue Res 187:1–24. https://doi.org/10.1007/BF00220615

Gnatzy W, Römer H (1980) Morphogenesis of mechanoreceptor and epidermal cells of crickets during the last instar, and its relation to molting-hormone level. Cell Tissue Res 207(1):41–57. https://doi.org/10.1007/BF00237885

Gnatzy W, Schmidt K (1971) Die Feinstruktur der Sinneshaare auf den Cerci von *Gryllus bimaculatus* Deg. (Saltatoria, Gryllidae). Z Zellforsch 122:190–209. https://doi.org/10.1007/BF00337629

Gnatzy W, Tautz J (1980) Ultrastructure and mechanical properties of an insect mechanoreceptor: Stimulus-transmitting structures and sensory apparatus of the cercal filiform hairs of Gryllus. Cell Tissue Res 213(2):441–463. https://doi.org/10.1007/BF00237890

Harley CM, English BA, Ritzmann RE (2009) Characterization of obstacle negotiation behaviors in the cockroach, *Blaberus discoidalis*. J Exp Biol 212:1463–1476. https://doi.org/10.1242/jeb.028381

Harris CR, Millman KJ, van der Walt SJ, Gommers R, Virtanen P, Cournapeau D, Wieser E, Taylor J, Berg S, Smith NJ, Kern R, Picus M, Hoyer S, van Kerkwijk MH, Brett M, Haldane A, Fernández del Río J, Wiebe M, Peterson P, Gérard-Marchant P, Sheppard K, Reddy T, Weckesser W, Abbasi H, Gohlke C, Oliphant TE (2020) Array programming with NumPy. Nature 585:357–362. https://doi.org/10.1038/s41586-020-2649-2

Heys JJ, Rajaraman PK, Gedeon T, Miller JP (2012) A Model of Filiform Hair Distribution on the Cricket Cercus. PLoS One 7:e46588. https://doi.org/10.1371/journal.pone.0046588

Honegger HW, Allgäuer C, Klepsch U, Welker J (1990) Morphology of antennal motoneurons in the brains of two crickets, *Gryllus bimaculatus* and *Gryllus campestris*. J Comp Neurol 291:256–268. https://doi.org/10.1002/cne.902910208

Honkanen A, Adden A, Da Silva Freitas J, Heinze S (2019) The insect central complex and the neural basis of navigational strategies. J Exp Biol 222:1–32. https://doi.org/10.1242/jeb.188854

Ifere NO, Shidara H, Sato N, Ogawa H (2022) Spatial perception mediated by insect antennal mechanosensory system. J Exp Biol 225:. https://doi.org/10.1242/jeb.243276

Ifere NO, Shidara H, Sato N, Ogawa H (2025) Identification of available travel paths' size and orientation by antennal mechanosensory system of crickets. J Insect Physiol 163:104816. https://doi.org/10.1016/J.JINSPHYS.2025.104816

Jacobs GA, Theunissen FE (2000) Extraction of sensory parameters from a neural map by primary sensory interneurons. J Neurosci 20:2934–2943. https://doi.org/10.1523/JNEUROSCI.20-08-02934.2000

Jaske B, Lepreux G, Dürr V (2021) Input of hair field afferents to a descending interneuron. J Neurophysiol 126:398–412. https://doi.org/10.1152/jn.00169.2021

Krause AF, Dürr V (2004) Tactile efficiency of insect antennae with two hinge joints. Biol Cybern 91:168–181. https://doi.org/10.1007/s00422-004-0490-6

Krause AF, Dürr V (2012) Active tactile sampling by an insect in a step-climbing paradigm. Front Behav Neurosci 6:26302. https://doi.org/10.3389/fnbeh.2012.00030

Krishnan A, Prabhakar S, Sudarsan S, Sane SP (2012) The neural mechanisms of antennal positioning in flying moths. J Exp Biol 215:3096–3105. https://doi.org/10.1242/jeb.071704

Lottem E, Azouz R (2009) Mechanisms of tactile information transmission through whisker vibrations. J Neurosci 29:11686–11697. https://doi.org/10.1523/JNEUROSCI.0705-09.2009

Loudon C, Bustamante J, Kellogg DW (2014) Cricket antennae shorten when bending (*Acheta domesticus* L.). Front Physiol 5:242. https://doi.org/10.3389/fphys.2014.00242

McCarter MG, Loudon C (2025) The spatial arrangement of Böhm's bristles and resolution of joint position in cricket antennae (*Acheta domesticus*) (Orthoptera: Gryllidae). J Insect Sci 25:22. https://doi.org/10.1093/jisesa/ieaf039

Miller JP, Krueger S, Heys JJ, Gedeon T (2011) Quantitative characterization of the filiform mechanosensory hair array on the cricket cercus. PLoS One 6:e27873. https://doi.org/10.1371/journal.pone.0027873

Mongeau JM, Demir A, Lee J, Cowan NJ, Full RJ (2013) Locomotion- and mechanics-mediated tactile sensing: antenna reconfiguration simplifies control during high-speed navigation in cockroaches. J Exp Biol 216:4530–4541. https://doi.org/10.1242/jeb.083477

Mongeau JM, Sponberg SN, Miller JP, Full RJ (2015) Sensory processing within cockroach antenna enables rapid implementation of feedback control for high-speed running maneuvers. J Exp Biol 218:2344–2354. https://doi.org/10.1242/jeb.118604

Moran DT (1971) Loss of the sensory process of an insect receptor at ecdysis. Nature 234:476–477. https://doi.org/10.1038/234476b0

Moran DT, Rowley JC 3rd, Zill SN, Varela FG (1976) The mechanism of sensory transduction in a mechanoreceptor. Functional stages in campaniform sensilla during the molting cycle. J Cell Biol 71(3):832–857. https://doi.org/10.1083/jcb.71.3.832

Murphey RK, Jacklet A, Schuster L (1980) A topographic map of sensory cell terminal arborizations in the cricket CNS: Correlation with birthday and position in a sensory array. J Comp Neurol 191:53–64. https://doi.org/10.1002/cne.901910103

Nelson ME, MacIver MA (2006). Sensory acquisition in active sensing systems. Journal of Comparative Physiology A, 192, 573–586. https://doi.org/10.1007/s00359-006-0099-4

Nishino H, Nishikawa M, Yokohari F, Mizunami M (2005) Dual, multilayered somatosensory maps formed by antennal tactile and contact chemosensory afferents in an insect brain. J Comp Neurol 493:291–308. https://doi.org/10.1002/cne.20757

Ogawa H, Mitani R (2015) Spatial dynamics of action potentials estimated by dendritic Ca2+ signals in insect projection neurons. Biochem Biophys Res Commun 467:185–190. https://doi.org/10.1016/j.bbrc.2015.10.021

Okada J, Toh Y (2000) The role of antennal hair plates in object-guided tactile orientation of the cockroach (*Periplaneta americana*). J Comp Physiol A Sensory, Neural, Behav Physiol 186:849–857. https://doi.org/10.1007/s003590000137

Okada J, Toh Y (2001) Peripheral representation of antennal orientation by the scapal hair plate of the cockroach *Periplaneta americana*. J Exp Biol 204:4301–4309. https://doi.org/10.1242/jeb.204.24.4301

Okada J, Toh Y (2004) Antennal system in cockroaches: a biological model of active tactile sensing. Int Congr Ser 1269:57–60. https://doi.org/10.1016/j.ics.2004.05.014

Okada J, Toh Y (2006) Active tactile sensing for localization of objects by the cockroach antenna. J Comp Physiol A 192:715–726. https://doi.org/10.1007/s00359-006-0106-9

Orenic TV, Held LI, Paddock SW, Carroll SB (1993) The spatial organization of epidermal structures: hairy establishes the geometrical pattern of *Drosophila* leg bristles by delimiting the domains of achaete expression. Development 118:9–20. https://doi.org/10.1242/dev.118.1.9

Prescott T, Diamond ME, Wing AM (2011). Active touch sensing. Philos Trans R Soc B 366:2989–2995. https://doi.org/10.1098/rstb.2011.0167

Pringle JWS (1938) Proprioception in insects: I. A new type of mechanical receptor from the palps of the cockroach. J Exp Biol 15:101–113. https://doi.org/10.1242/jeb.15.1.101

R Core Team (2025) R: a language and environment for statistical computing. R Foundation for Statistical Computing, Vienna. https://www.r-project.org/

Ritzmann RE, Harley CM, Daltorio KA, Tietz BR, Pollack AJ, Bender JA, Guo P, Horomanski AL, Kathman ND, Nieuwoudt C, Brown AE, Quinn RD (2012) Deciding which way to go: how do insects alter movements to negotiate barriers? Front Neurosci 6:97. https://doi.org/10.3389/fnins.2012.00097

Schafer R (1997) Postembryonic development in the antenna of the cockroach, *Leucophaea maderae*: Growth, regeneration, and the development of the adult pattern of sense organs. J Exp Zool 183(3):353–364. https://doi.org/10.1002/jez.1401830309

Schafer R, Sanchez TV (1973) Antennal sensory system of the cockroach *Periplaneta americana*: Postembryonic development and morphology of the sense organs. J Comp Neurol 149(3):335–353. https://doi.org/10.1002/cne.901490304

Schneider CA, Rasband WS, Eliceiri KW (2012) NIH Image to ImageJ: 25 years of image analysis. Nat Methods 9:671–675. https://doi.org/10.1038/nmeth.2089

Schütz C, Dürr V (2011) Active tactile exploration for adaptive locomotion in the stick insect. Philos Trans R Soc B Biol Sci 366:2996–3005. https://doi.org/10.1098/rstb.2011.0126

Shimozawa T, Kanou M (1984) Varieties of filiform hairs: range fractionation by sensory afferents and cereal interneurons of a cricket. J Comp Physiol A 155:485–493. https://doi.org/10.1007/BF00611913

Staudacher EM, Gebhardt M, Dürr V (2005) Antennal movements and mechanoreception: neurobiology of active tactile sensors. In: Adv Insect Physiol 32:49–205. https://doi.org/10.1016/S0065-2806(05)32002-9

Straka H, Simmers J, Chagnaud BP (2018) A new perspective on predictive motor signaling. Curr Biol 28:R232–R243. https://doi.org/10.1016/j.cub.2018.01.033

Strauß J (2024) Early postembryonic morphology of the stick insect subgenual organ complex. Biologia 79:3129–3136. https://doi.org/10.1007/s11756-024-01758-7

Suzuki AC, Nishimura K (1997) The Testis Development in 3rd- to 6th-Instar Nymphs of the Cricket, *Gryllus bimaculatus*. Zoolog Sci 14:637–639. https://doi.org/10.2108/zsj.14.637

Thomann M, Seifert P, Altner H (1997) Moulting of mechanoreceptive hair sensilla of *Lepisma saccharina* (Zygentoma) and *Machilis* spec. (Archaeognatha). Tissue Cell 29(4):421–430. https://doi.org/10.1016/S0040-8166(96)80039-5

Toh Y (1977) Fine structure of antennal sense organs of the male cockroach, *Periplaneta americana*. J Ultrastruct Res 60:373–394. https://doi.org/10.1016/S0022-5320(77)80021-X

Toh Y (1981) Fine structure of sense organs on the antennal pedicel and scape of the male cockroach, *Periplaneta americana*. J Ultrastruct Res 77:119–132. https://doi.org/10.1016/S0022-5320(81)80036-6

Virtanen P, Gommers R, Oliphant TE, Haberland M, Reddy T, Cournapeau D, Burovski E, Peterson P, Weckesser W, Bright J, van der Walt SJ, Brett M, Wilson J, Millman KJ, Mayorov N, Nelson ARJ, Jones E, Kern R, Larson E, Carey CJ, Polat I, Feng Y, Moore EW, VanderPlas J, Laxalde D, Perktold J, Cimrman R, Henriksen I, Quintero EA, Harris CR, Archibald AM, Ribeiro AH, Pedregosa F, van Mulbregt P, SciPy 1.0 Contributors (2020) SciPy 1.0: fundamental algorithms for scientific computing in Python. Nat Methods 17:261–272. https://doi.org/10.1038/s41592-019-0686-2

Watanabe T, Ugajin A, Aonuma H (2018) Immediate-early promoter-driven transgenic reporter system for neuroethological research in a hemimetabolous insect. eNeuro 5:e0061-18.2018. https://doi.org/10.1523/ENEURO.0061-18.2018

Yoritsune A, Aonuma H (2012) The anatomical pathways for antennal sensory information in the central nervous system of the cricket, *Gryllus bimaculatus*. Invertebr Neurosci 12:103–117. https://doi.org/10.1007/s10158-012-0137-6

Zweifel NO, Hartmann MJZ (2020) Defining active sensing through an analysis of sensing energetics: homeoactive and alloactive sensing. J Neurophysiol 124:40–48. https://doi.org/10.1152/jn.00608.2019

Research Achievement

Publication

1. **Lyu, H.** and Ogawa, H. (2026) Functional spatial organization of antennal hair plate sensilla and their development in crickets. Cell and Tissue Research 404: 10. https://doi.org/10.1007/s00441-026-04073-6
2. **Lyu, H.** and Ogawa, H. (2025) Developmental changes in the morphology and three-dimensional arrangement of antennal hair plates in crickets. bioRxiv 2025.12.10.693584. https://doi.org/10.64898/2025.12.10.693584

Presentations

International

1. **Lyu, H.** and Ogawa, H. Developmental changes in the morphology and three-dimensional arrangement of the antennal hair plates in crickets. 55th Annual Meeting of the Society for Neuroscience. [PSTR229.09], San Diego, USA. November 2025. (Virtual Poster)

Domestic

1. **呂 惠**，小川 宏人．コオロギ触角基部の毛板機械感覚子の形態と 3 次元的配置の発達変化．日本動物学会第 96 回大会 [P121A] 名古屋，2025 年 9 月（ポスター発表）
2. **呂 惠**，小川 宏人．Neural representation of spatial information mediated by cricket antennal mechanosensory system. 日本比較生理生化学会第 45 回大会 [P2-15] 大阪，2023 年 12 月（ポスター発表）

Achievements of other research

Publication

1. **Lyu, H.** and Mizunami, M. (2022) Conditioned taste aversion in the cricket *Gryllus bimaculatus*. Scientific Reports 12: 1–8. https://doi.org/10.1038/s41598-022-13500-x

Acknowledgements

As I write the final chapter of this dissertation, I find myself reflecting on the journey that has brought me to the end of my doctoral studies. This accomplishment would not have been possible without the unwavering support and guidance of my supervisor, family and colleagues.

First and foremost, I owe my deepest gratitude to my supervisor, Prof. Hiroto Ogawa, for his exceptional mentorship and constant support throughout my Ph.D. Despite his demanding schedule, he always made time to respond to my questions with patience and care. His insightful guidance helped me clarify my thoughts and shaped the direction of my research, ultimately making this dissertation possible. Prof. Ogawa provided indispensable technical and logistical support, generously offering the equipment and research environment essential for conducting my experiments. Beyond these practical contributions, I have greatly benefited from his emphasis on meticulous observation and thoughtful interpretation of experimental data, which have had a lasting influence on my scientific outlook and approach. I am deeply indebted to him for his kind understanding and encouragement during my one-year leave for childbirth and childcare. His warm support enabled me to resume my research with renewed confidence and to achieve a meaningful balance between academic pursuit and family life.

I would like to express my heartfelt gratitude to my family. During the course of my doctoral studies, I experienced several significant events in my life, including the global pandemic, an international marriage, the passing of my father, and the birth of my child. The unwavering support and encouragement from my family have been an inexhaustible source of strength and motivation, helping me withstand difficulties and challenges without being overcome by them. In times of uncertainty and doubt, their love and understanding have given me the resilience and comfort I needed to keep moving forward.

I would like to express my sincere appreciation to Prof. Kazuhiro Wada and Prof. Nobuaki Tanaka for reviewing my doctoral thesis and providing helpful comments. I am also grateful to all members of the Ogawa Lab for their constructive feedback and continuous support. Special thanks go to Dr. Matasaburo Fukutomi and Mr. Hikaru Chida for their valuable advice on statistical analysis methods.

I deeply appreciate the members of the Behavioral Neurobiology Group at Hokkaido University for their insightful comments and stimulating discussions. In particular, I would like to thank Prof. Masayo Soma, Prof. Yuichi Takeuchi, and Prof. Tomomi Tsunematsu for their thoughtful suggestions and expert advice.

Lastly, I gratefully acknowledge the financial support from the Japan Science and Technology Agency (JST), SPRING Grant No. JPMJSP2119.